A REPORT ON

Assessment of stormwater infrastructure for mitigating flooding and non-point source pollution

PREPARED FOR:

TEXAS GENERAL LAND OFFICE

AUSTIN, TEXAS

PREPARED BY:

YU ZHANG, PHD
HELIA FARZANEH, NABIN BASNET, AND
MOHAMMADVAGHEF GHAZVINIAN
DEPARTMENT OF CIVIL ENGINEERING
UNIVERSITY OF TEXAS AT ARLINGTON
ARLINGTON, TEXAS 76019

QIN QIAN, PHD
DEPARTMENT OF CIVIL & ENVIRONMENTAL ENGINEERING
LAMAR UNIVERSITY,
BEAUMONT, TEXAS 77705

JANUARY 2022

A report funded by a Texas Coastal Management Program Grant approved by the Texas Land Commissioner pursuant to National Oceanic and Atmospheric Administration Award No. NA19NOS4190106.

TABLE OF CONTENTS

LIST OF TABLES

LIST OF FIGURES

EXECUTIVE SUMMARY

Flooding is the top natural hazard impacting coastal and inland communities in Texas. In many coastal regions, flooding contributes to the increased aquatic contaminants in estuaries and offshore water bodies. The lower Neches River valley is among the regions that saw increasing risk of flooding and water quality problems in recent years. The region was the epicenter of Hurricane Harvey of 2017 and Tropical Imelda of 2019, and experienced water quality problems ranging from excessive sedimentations to elevated fecal bacteria load. In particular, fecal bacteria load has been observed to be on the rise over the past two decades. Since 2009, bacteria concentration at the Neches River Tidal has frequently been found to be above the US EPA recommended threshold, posing a threat to public health. The source of the contamination remains unclear, yet leakage from on-site sewage facilities (OSSFs) along the northeastern side of the river is seen as one of the most probable contributing sources.

A research team consisting of investigators from UT Arlington and Lamar University conducted a study to examine possible measures to alleviate the flooding and water quality issues along the lower Neches River. The study was supported by the Texas General Land Office Coastal Management Project (CMP) Cycle 24 fund and focused on the 20 miles of the Neches River from the confluence of Pine Island Bayou to the intersection of Interstate Highway 10. Specifically, the project appraises the feasibility and cost-effectiveness of employing stormwater best management practices (BMPs) along a major tributary of the Neches River Tidal as a means for mitigating flooding and excessive bacteria loading in the latter. The research team established a coupled modeling system by combining the EPA Stormwater Management Model (SWMM) and Micro-Organism Prediction in Urban Stormwater (MOPUS) model, and applied this system to assess and anticipate the cost-effectiveness of BMPs in reducing the volume of flow into Neches and bacteria loading. The primary BMP type implemented in the modeling system is wet detention pond which has been shown to be effective in reducing bacteria concentration. In order to determine the costs and impacts of BMP implementation, an ensemble of scenarios were created, each incorporating a specific, hypothetical spatial distribution of wet detention ponds across the subcatchments along the said tributary to Neches River Tidal. Given the possible primacy of OSSFs as contributors to the bacteria load, the BMPs were preferentially implemented over the subcatchments that feature higher concentration of OSSFs for physical realism. The modeling

system that implements these scenarios was used to simulate streamflow and bacteria loading when forced by 24-h design storms with averaged recurrence intervals of 25, 50 and 100 years. These design storms were developed from NOAA Atlas-14 Intensity-Duration Frequency curves for this region. In each scenario, the density of hypothetical BMPs was allowed to vary to achieve ~40% reduction in flow for each design storm relative to the status quo (no implementation of BMPs), and the costs associated with the implementation were calculated for each scenario.

The outcome of simulations using the coupled SWMM-MOPUS modeling framework indicates that in order to achieve ~40% of reduction in flow, the aggregate area of detention ponds needs to reach 1 – 3 percent of total area of the subcatchment. In addition, the reduction in flow roughly translates into reduction in 30-40% reduction in bacteria load. The total costs associated with constructing the BMPs range within $13-33 million for the 25-year storm, $16-40 million for 50-year storm, and $19-45 million for 100-year storm. It should be noted that the accuracy of these estimates is predicated on the assumptions underlying the model framework, and recommendations are made on gathering additional, specific data sets to calibrate and validate the model simulations, including flow observations along the mainstem of lower Neches River and its tributary, samples of bacteria in the upstream of the tributary and adjacent to the OSSFs, and the empirical data on differential roles of vegetations in detention ponds in regulating the removal of fecal bacteria.

1. INTRODUCTION AND PROBLEM STATEMENT

Flooding has consistently ranked as the most dangerous natural hazard for coastal and inland areas in southeast Texas, and more specifically Jefferson and Orange Counties that are situated to the east of Houston (Blake and Zelinsky 2017). During the last decade, incidence of floods and concomitant water quality issues has been on the rise in the region. Over the past five years alone, the region experienced major floods including the June flood of 2015, Tax Day flood of 2016, Hurricane Harvey of 2017, and Tropical Storm Imelda of 2019. These floods have caused many fatalities and billions of dollars in damages along the southeast Texas coast. Adding to the woes, flash floods brought by localized intense rainfall attributed to a mix of tropical, convective and frontal systems are becoming increasingly frequent. These floods damage infrastructures, interrupt transportation, and disrupt local and regional economies; moreover, floodwater runs over land, washes off sediments, oxygen-demanding substances, pathogens, and toxins into streams which then carry these to bays and estuaries, causing deterioration of water quality off the coast (Edward 2021).

After Harvey, there is a widening consensus that rising sea surface temperature in a warming climate has the potential of increasing the occurrence of storms and flooding along the Gulf Coast (Kossin, 2018), and this has broad implications on resilience of the community over the region. Federal, state, and local authorities have been seeking structural and non-structural mitigation measures aimed at alleviating the impacts of flooding and the ensuing water quality issues brought by the storms. Among these measures being considered are distributed stormwater Best Management Practices (BMPs), which range from detention/retention basins, constructed wetlands, pervious pavements, and vegetated swales. These BMPs have seen implementations in a number of coastal states; while not intended to be wholesale remedies for extreme flooding and associated water quality problems, they saw various degrees of successes in reducing the related impacts. Karamouz et al. (2020) utilize a combination of coastal protection strategies such as levees and constructed wetlands leads to significant improvement of flood reliability in Hunts Point WWTP located in New York City. Vis et al. (2003) compared the Netherlands' present flood risk management program, which includes a resistance strategy aimed at preventing flooding by elevating the dikes, and a resilience approach aimed at mitigating the impacts of these floods by permitting some flooding.

Within this region, the lower 20 miles of the Neches River from the confluence of Pine Island Bayou to the intersection of Interstate Highway 10 has gained much attention over recent years. Located immediately to the east of City of Beaumont (Fig. 1-1), this segment of Neches River has been the scene of intense flooding during Harvey. The storm brought much of the area under water; the city of Beaumont lost its pumping stations due to flooding and the Lower Neches River Authority's pumping station upstream of the Saltwater Barrier near the confluence with Pine Island Bayou was inundated and nearly went offline. Floodwater also unleashed enormous amounts of sediments and pollutants to the Neches River and the downstream Sabine Lake. Figure 1-1 shows the location of the study area which is a part of the Neches River Tidal segment (0601). This figure illustrates the map of the Assessment Unit of 0601-04 which starts below Kansas City Southern Railroad bridge and extend to saltwater barrier.

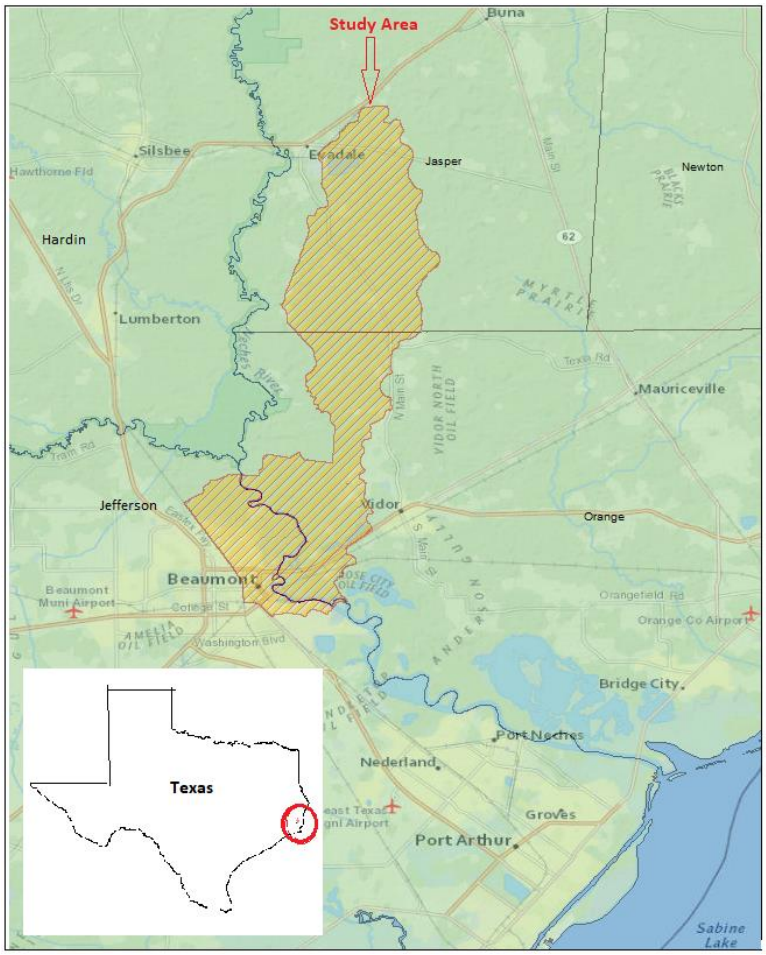

Figure 1-1. Overview map of the Assessment Unit of 0601-04 which starts below Kansas City Southern Railroad bridge and extend to saltwater barrier.

As shown in Figure 1-1, this segment of Neches River receives runoff from Neches River upstream, a part of Beaumont to the east of Eastern Freeway, and a sizeable tributary that originates in the Jasper County and joins the main stem of Neches to its east in Orange County. The drainage of interest thus overlaps with three counties (Jefferson, Orange, and Jasper County) and the city of Beaumont, with total drainage area 79.6 square miles. The breakdown of the area, population, and population density of each county in the study area are listed in Table 1-1.

Table 1-1. Demography of the study area by county

County Name	Area (mi^2)	Total Population (in 2010)	Population Density
Jasper County	970	35,710	37
Jefferson County	941	252,273	268
Orange County	343	81,837	239

As indicated earlier, this area has seen rising incidence of nuisance flooding in recent years, consistent with the rising trend of precipitation in the region (Nielsen-Gammon et al., 2020). Coincidental with the rise in precipitation and flooding, there is also a conspicuous upward trend in fecal bacterial loading in the Neches River Tidal (Figure 1-2).

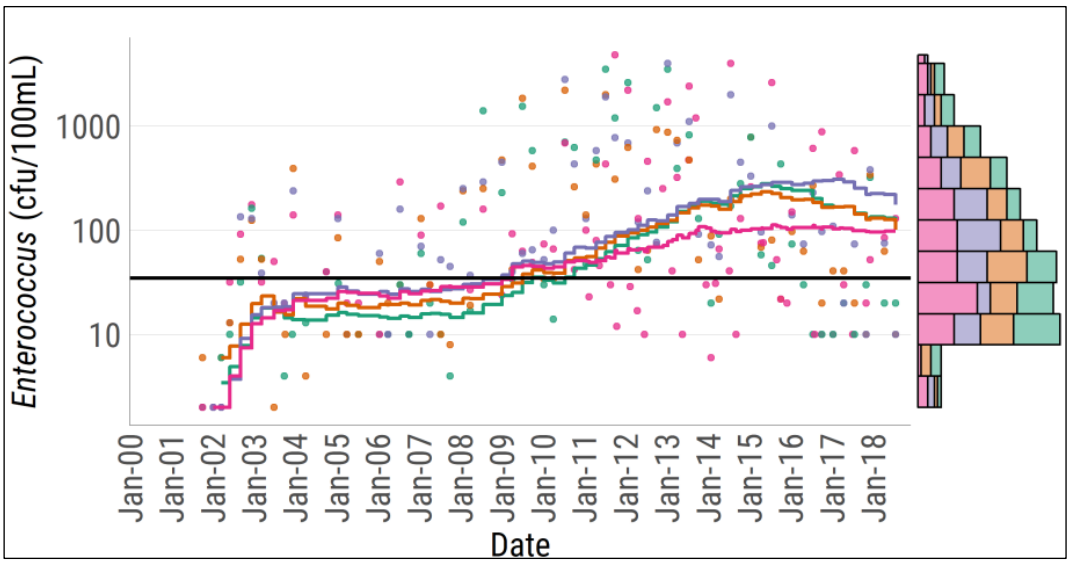

Source: Texas Water Research Institute

Figure 1-2. Summary plots of historical bacteria datasets for degraded AUs in Neches River Tidal (0601) from June 2003 to December 2018.

As seen in Figure 1-2, concentration of Enterococcus from samples taken at four assessment units along the main stem of Neches has risen sharply since the mid-2000s. The curves with pink, orange, green, and purple colors show the trend line of historical bacteria (Enterococcus) concentration for different Assessment Units (AUs) of 0601-01, 0601-02, 0601-03, and 0601-04 in Neches River Tidal segment (0601). The histogram in the right side of Figure 1-2 indicates the probability distribution of each specific Enterococcus concentration within different AUs of the Neches River Tidal segment. From 2010 onward, the concentration has often exceeded 35 cfu/100 ml that is the EPA recommended bacteria threshold for contact recreation. The processes that give rise to the upward trend in Enterococcus are not yet clear, but the research done by the project team suggests that seepage from on-site sewage facilities (OSSFs) is a major culprit. Over the region, the city of Beaumont maintains a centralized sewage system, whereas communities in Orange County still rely on the OSSFs. Figure 1-3 shows the locations of OSSFs in the study watershed.

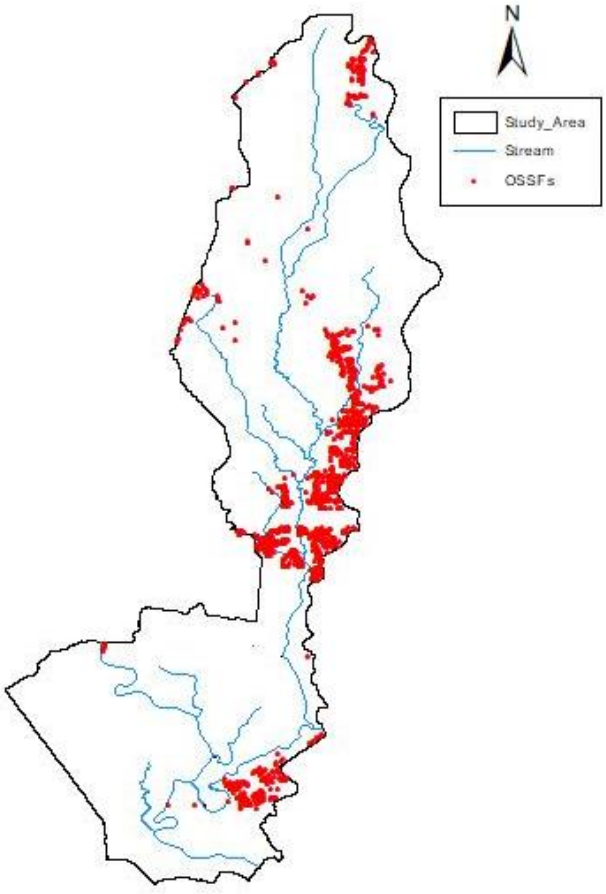

Figure 1-3. Locations of on-site sewage facilities (OSSFs) in the study watershed.

Failures of OSSFs can often be triggered by flooding, and they tend to become more frequent as the systems age (Reed, Stowe, and Yanke, 2001). While it is yet unknown the exact locations where failures occur or their proportional contribution to the presence of Enterococcus, it is prudent to devise mitigation measure to target the sub-drainages with higher density of OSSFs.

To address the rising threats of flooding and water quality degradation to the region, the UTA-Lamar University research team undertook a study between October 2019 and December 2021 to examine the potential of deploying a large number of distributed stormwater best management practices as a mitigation mechanism. The study was supported by the Texas General Land Office Coastal Management Program (CMP), and was intended to achieve three important objectives, namely 1) providing an up-to-date assessment of flood risks along the study reach using the latest precipitation frequency maps; 2) identifying stormwater BMPs that hold the most promises in alleviating the flooding and water quality problems; and 3) obtaining quantitative estimates of expected reduction in the flow and bacteria loading with the implementation of BMPs and associated costs using a coupled stormwater management-bacteria life cycle model. In these regards, the NOAA Atlas-14 precipitation frequency estimates (Perica et al., 2018) were used to derive 24-h design storms, which were in turn used to drive Stormwater Management Model (SWMM) implemented for the study watershed. To estimate the range of costs and impacts of BMP implementations, an ensemble of scenarios, each with a prescribed spatial distribution of conceptual BMPs, were incorporated in the SWMM implementation. The costs associated with each hypothetical scenario were estimated by following guidelines from EPA and using cost estimates for projects carried out in other parts of the nation. The runoff series obtained from SWMM simulations without and with the BMPs were fed to the Micro-Organism Prediction in Urban Stormwater (Hou et al., 2019) model that calculates the changes in the bacteria loading.

The study was conducted in close coordination with regional partners include the Lower Neches Valley Authority, the city of Beaumont, and the Texas Water Research Institute (TWRI). It leverages outcomes from extant efforts undertaken to create the Total Maximum Daily Load (TMDL) for the study watershed but goes beyond the latter work in that a) it integrates a bacteria life cycle model for simulating the concentration of bacteria in streams rather than relying on load-duration curves; and b) it explores the use of BMPs as a strategy for alleviating the water quality problems. In addition, the cost-benefit analysis performed in this study will help regional partners,

including the city of Beaumont, Jefferson and Orange Counties in planning on the adoption of BMPs. Though the study focuses on the communities situated within the specific locality, the decision framework thus established can be widely applied to other coastal communities to assess the potential benefits to be derived from implementing similar stormwater BMPs.

The rest of the report is divided into three sections. Section 2 describes the methodology, modeling systems, and data. Section 3 presents the design storms and simulations of the coupled model. Section 4 summarizes the lessons learned and offers recommendations.

2. METHODOLOGY

2.1 Overview of coupled modeling system

The coupled modeling system that we established for the study region consists of a runoff/water quality model implemented using EPA's Stormwater Management Model (SWMM) platform, and the Micro-Organism Prediction in Urban Stormwater (MOPUS) model. Figure 2-1 depicts a schematic of a coupled 1system that incorporates both the SWMM and MOPUS models.

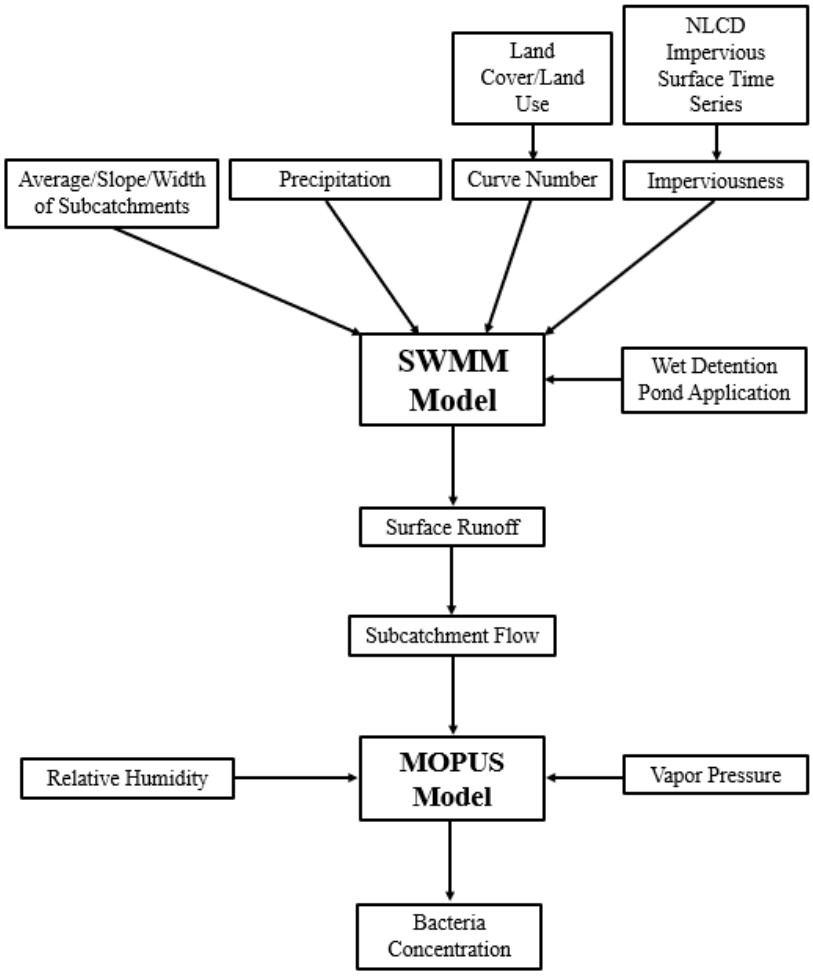

Figure 2-1. A schematic of the integration of SWMM and MOPUS models

The SWMM was developed by USEPA for simulating stormwater runoff primarily for urban/suburban lands; its first version was released in 1971 and it has undergone several major

upgrades. The latest version (5.1.013) was employed in this study. The modeling system is capable of performing runoff and water quality simulation for a variety of land cover types either for a specific event or in a continuous mode. The current version of SWMM model offers functions to simulate both surface runoff and discharge from groundwater into the drainage system. It also contains a rich set of modules for simulating pollutant washoff, buildup, sanitary flows, and impacts of BMPs. As our purpose is to determine the runoff over major storm events, groundwater contribution is assumed to be minor and only the overland flow module is implemented in this study.

Jang et al.2007 employed the SWMM model to control urban runoff before to and after urban growth in four South Korean areas. A comparison of the findings with those from prior studies conducted in the same area shown that the SWMM model is capable of incorporating many models, such as the shorter and longer length of the discharge peak for post-development settings (Jang et al. 2007). Park et al. used the SWMM model to simulate the flow hydrograph and volume of pollutant loads in order to examine the impact of watershed segmentation and geographical isolation of South Korea's sewage drainage network. The findings indicated that the model accurately predicted peak discharge and runoff volume, and that the influence of spatial resolution on surface runoff outcomes was minimal (Park et al. 2008). Wang et al. used the SWMM model to analyze and simulate runoff mitigation techniques. They examined three scenarios including permeable pavement, rain collection, and a green roof and concluded that permeable pavement was the most effective strategy for reducing runoff volume, reducing runoff by around 30%. (Wang et al. 2017).

SWMM uses subcatchment as the basic computational unit for runoff calculation. These subcatchments are connected through conduits (channels or pipelines). For calculating runoff from rainfall, SWMM provides three options, i.e., Horton, Green-Ampt, and SCS Curve Number method. The runoff computed for each subcatchment is routed through conduits (channels or pipes). There are several routing schemes implemented in SWMM, including steady flow, kinematic wave, steady flow, and full dynamic wave (James & Ferguson, 2020). The model can explicitly represent eight types of BMPs, i.e., biorentention cells, rain gardens, green roofs, infiltration trenches, continuous permeable pavement, rain barrels, rooftop disconnection, and vegetative swales. The SWMM model configuration will be described in detail in Section 2.2.

The MOPUS model was developed by McCarthy et al. (2011) to simulate E. coli levels in stormwater subcatchments using a precipitation-runoff model and a micro-organism model. In this study, the MOPUS model underwent enhancements to yield the MOPUS_S that allows the model to integrate simulated runoff from the SWMM and account for variations in microbial sources among subcatchments. These enhancements will be discussed in Section 2.3.

The coupled SWMM-MOPUS_S model thus established served as the tool for evaluating the cost-efficacy of BMPs under an ensemble of scenarios, each with a prescribed distribution of BMP implementations and hypothetical design storms. In each scenario, the 1-day design hyetograph served as the input forcing to SWMM that generates simulated runoff series for each subcatchment, and these series were ingested into the MOPUS_S to estimate reduction in bacteria loading as a result of BMP implementation. The design storms were constructed following standard engineering practice which involves the creation of design hyetographs from pointwise precipitation frequency estimates for 24-h duration from NOAA Atlas-14. The scenarios of BMP implementations and underlying considerations will be discussed in Section 2.4. The procedure for generating the design storms will be presented in Section 2.5.

2.2 SWMM configuration

In order to configure SWMM and derive model parameters, the team gathered a wide range of GIS data sets over the region, comprising current soil type, land use/land cover, infiltration properties, and hydrograph. The data sources are summarized in Table 2-1.

Table 2-1. Information of the data sources.

Data	Source
Precipitation	https://water.weather.gov/precip/
National Hydrography Data (NHD)	https://www.usgs.gov/national-hydrography/access-national-hydrography-products
Multiresolution Land Characteristics	https://www.mrlc.gov/data
Soil Database	https://catalog.data.gov/dataset/soil-survey-geographic-database-ssurgo
Vapor Pressure and Relative Humidity	https://nsrdb.nrel.gov

In our SWMM implementation, the drainage of interest is subdivided into 11 subcatchments to enable spatially distributed siting of hypothetical BMPs and thus allow for a detailed assessment of the impacts from spatial variations of BMPs on flow and bacteria loading. In order to delineate these watersheds, watershed boundary and digital elevation data from NHD-Plus2 data set were used. The former was used to identify the drainage that contributes to the study segment of Lower Neches River, whereas the latter was used to derive boundaries for the subcachments. The geographic extents of these subcatchments thus derived and their representations in SWMM are shown in Figure 2-2.

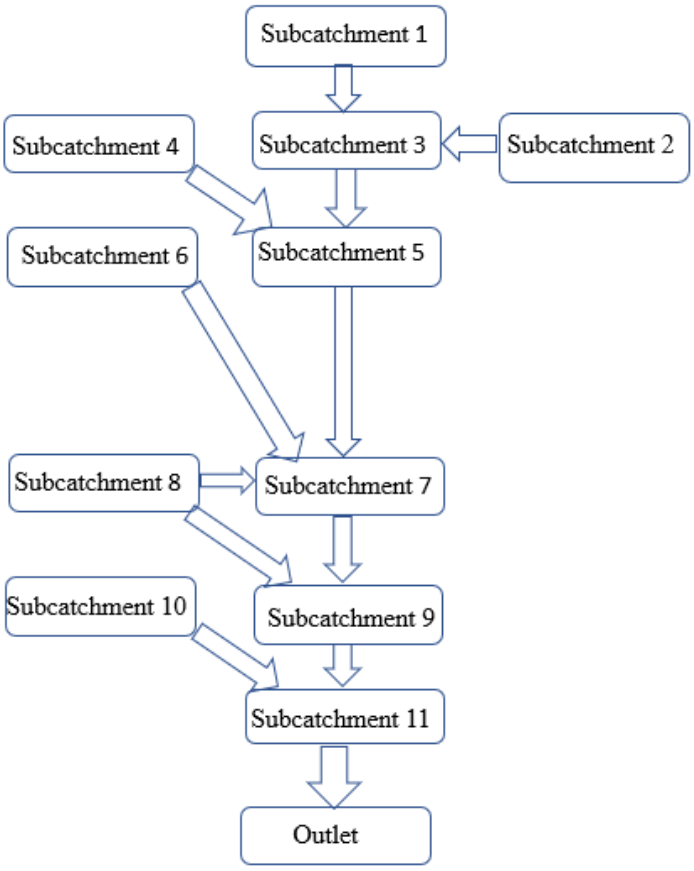

Figure 2-2. The Schematic locations of the subcatchments in SWMM.

In SWMM, a subcatchment serves as the basic unit in which runoff is computed from rainfall excess; the runoff reaches the subcatchment outlet via overland flow. In simulating runoff, SWMM divides each subcatchment into pervious and impervious surfaces, and only calculates infiltration over the pervious surface. The model offers several options for modeling infiltration,

out of which the SCS curve number option was chosen due to the presence of an established approach for estimating the curve from land cover and soil type. This approach requires parameters including the curve number, drainage area, and percentage imperviousness. The model also offers an option to model depression storage, but for simplicity this storage was assumed to be zero. To calculate overland flow, SWMM requires the specification of flow length, slope, flow width, and Manning's N for each subcatchment. The processes through which these parameters were estimated are briefly described below.

For each subcatchment, the percentage impervious surface parameter was specified according to the land cover composition, and the SCS curve number was estimated using curve number from land cover and soil drainage properties. The land cover used in this study was taken from 2016 National Land Cover Database (NLCD), and a map of land cover is shown in Figure 2-3.

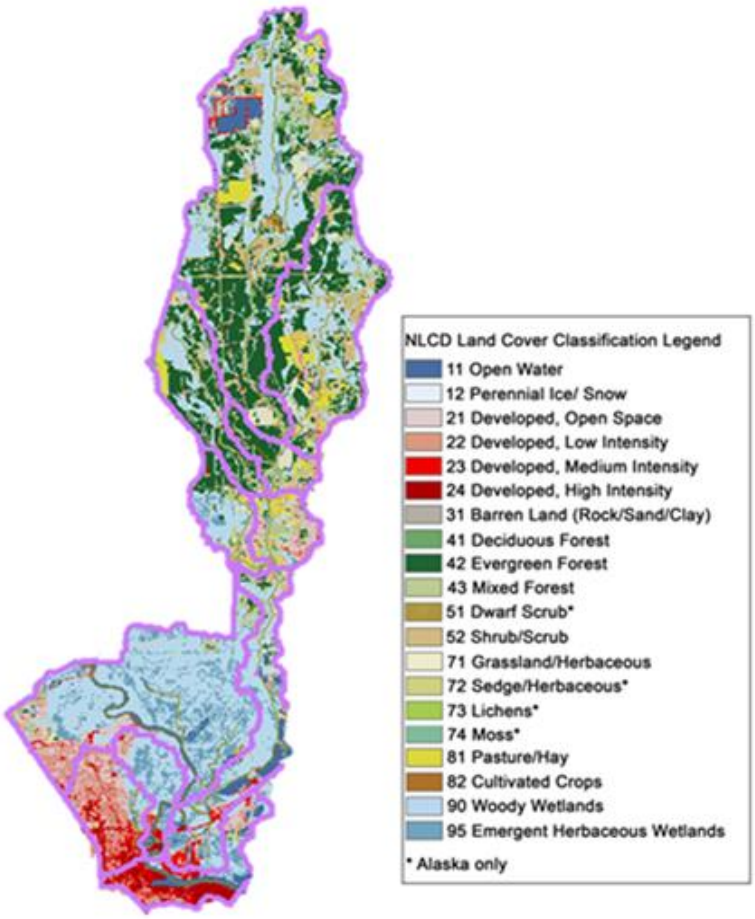

Figure 2-3. Illustration of the NLCD Land Cover Classification within the Neches River watershed.

The Lower Neches River watershed features large areas of wetlands and open water. The amount of forested land increases in the northern portion of the watershed that overlaps with the Big Thicket Reserve (Figure 2-3**Error! Reference source not found.**). As shown in Table 2-2, this watershed has around 17 percent developed land, with the other 27 percent consisting mostly of evergreen and mixed forest.

Table 2-2. Land Cover summary of Neches River watershed.

Land Cover	Acres	Percent of Total
Woody Wetlands	16,546	32.5
Evergreen Forest	10,770	21.1
Emergent Herbaceous Wetlands	3,508	6.9
Developed, Open Space	3,177	6.2
Mixed Forest	3,081	6
Developed, Low Intensity	3,061	6
Shrub/ Scrub	2,819	5.5
Open Water	2,125	4.2
Hay/Pasture	1,659	3.3
Herbaceous	1,427	2.8
Developed, Medium Intensity	1,223	2.4
Developed, High Intensity	1,134	2.2
Barren Land	212	0.4
Deciduous Forest	123	0.2
Cultivated Crops	79	0.2
Total	50,943	100

The soil hydraulic properties used in this study were derived from the Natural Resources Conservation Service (NRCS) SSURGO database. The drainage properties fall into four major classes (A, B, C and D), and three dual classes (A/D, B/D, and C/D). These classes are determined by the expected rate of water infiltration when soils are not covered by vegetation, are moist, and receive precipitation from storms that last for an extended period. Figure 2-4**Error! Reference source not found.** depicts the spatial distribution of soil hydrologic groups throughout the study watershed. It is evident that the upstream is dominated by moderately-poorly drained soils, and this highlights the importance of retention as a strategy for reducing runoff over the region.

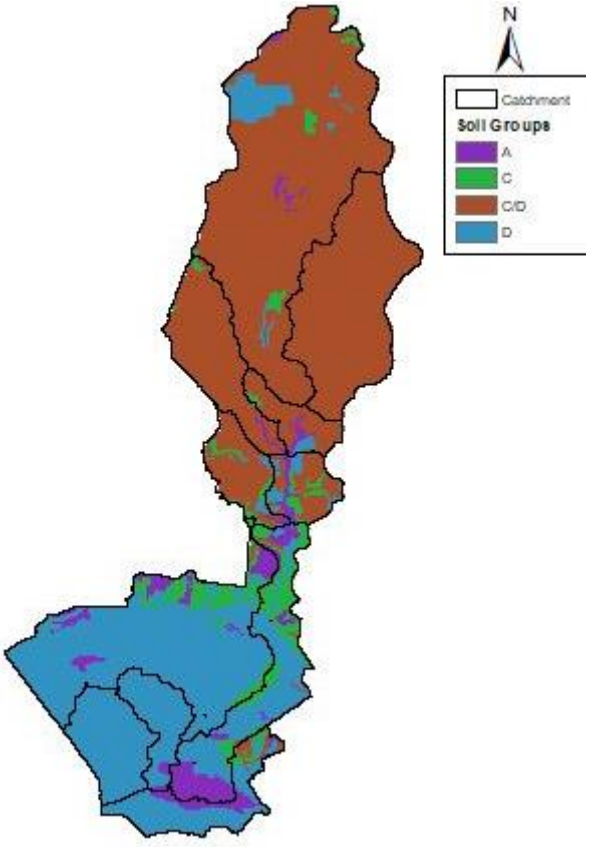

Figure 2-4. Illustration of the soil hydrologic group within the Neches River watershed.

The averaged slope for each subcatchment was calculated by taking an average of slope values computed from 30-m Digital Elevation Model as described in equation (2-1). This results in an averaged slope of 3%.

$$\text{Slope (\%)} = \left(\frac{H}{d}\right) * 100; \text{ where } H = \text{elevation (ft) and } d = \text{distance (ft)} \quad (2\text{-}1)$$

For each subcatchment, the width of the subcatchment was estimated by measuring the length of an overland flow path using the DEM map in ArcGIS. According to the manual, the width of a subcatchment is computed by dividing the area of each subcatchment by the length of the overland flow, as shown in equation **Error! Reference source not found.**.

$$\text{Width (\%)} = \left(\frac{A}{D_{OF}}\right); \text{ where } A = \text{area (ft}^2\text{) and } D_{OF} = \text{Longest overland flow length (ft)} \quad (2\text{-}2)$$

In this equation, the longest flow path was computed for each subcatchment.

The values of SWMM parameters for infiltration and routing calculation for each subcatchment are shown in Table 2-3.

Table 2-3. Parameter values for infiltration and overland flow calculations.

Subcatchment	Area (mi^2)	Flow length (mi.)	Width (ft)	Curve Number	% Imperviousness
1	23.31	11.81	1.97	85	1.77
2	10.87	5.13	2.12	84	1.37
3	5.35	6.00	0.89	84	0.69
4	2.08	2.78	0.75	81	2.07
5	2.39	2.10	1.14	83	7.89
6	2.87	6.00	0.47	88	1.32
7	7.15	9.84	0.73	95	6.07
8	15.4	6.00	2.56	96	0.21
9	2.37	2.72	0.98	88	39.70
10	3.91	2.30	1.70	73	9.17
11	3.92	2.66	1.47	94	38.92

The channel flow routing is performed using the kinematic wave routing for its computational efficiency, and its ability to account for temporal variation in flow rate as well as nonlinear dependence of wave celerity on discharge. The kinematic wave routing requires the specification of Manning's n for the channel. In this study, the Manning's n was treated as a calibration parameter.

A primary challenge in implementing SWMM is the lack of stream gauges station within the study watershed. To address this, calibration was instead performed over a nearby "surrogate" watershed with gauged flow record, Cow Bayou near Mauriceville, Texas (USGS ID: 08031000), which is located to the east of the study watershed (Figure 2-5) and has a drainage area of 88.9 square miles.

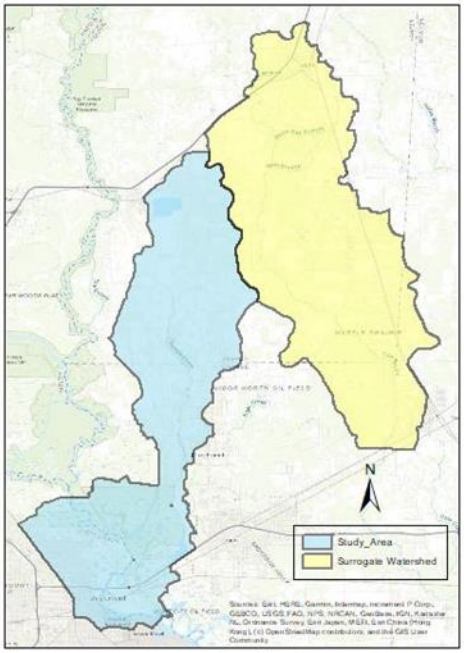

Figure 2-5. The Schematic locations of the area of interest and test catchment.

The physiographic properties of the watershed are summarized in Table 2-4.

Table 2-4. Physical characteristics of the surrogate watershed in SWMM.

Physical characteristics in SWMM	Value
Area (ha)	23050
Width (m)	500
Slope (%)	2
Imperviousness	50
Curve Number	80

It was surmised that the parameter values for the surrogate and study watersheds are comparable given geographic proximity and similarity in land cover/soil. Manual calibration is performed for the Cow Bayou watershed (highlighted in yellow in Figure 2-1) in which the Manning's n have been adjusted to allow the simulated discharge to closely mimic the observed flow data. Then the resulting parameter values are transferred to all subcatchments in the study watershed. Calibration for this surrogate watershed resulted in the determination of the manning's n for overland flow on both impervious and pervious region, which offers a range for each of them. The determined range's average value is used to indicate the manning's n for both impervious and

pervious section within each subcatchment of the area of interest. It should be noted that, the calibration is conducted for the time intervals of 10/1/2002 to 10/31/2002, 3/1/2016 to 3/31/2016, and 4/1/2016 to 4/30/16. The average manning's values of the previous and impervious areas are estimated at 0.2 and 0.07, respectively. Figure 2-6**Error! Reference source not found.** illustrates the observed and simulated flow comparison to obtain the manning's roughness coefficient for pervious and impervious surfaces for three proposed time intervals.

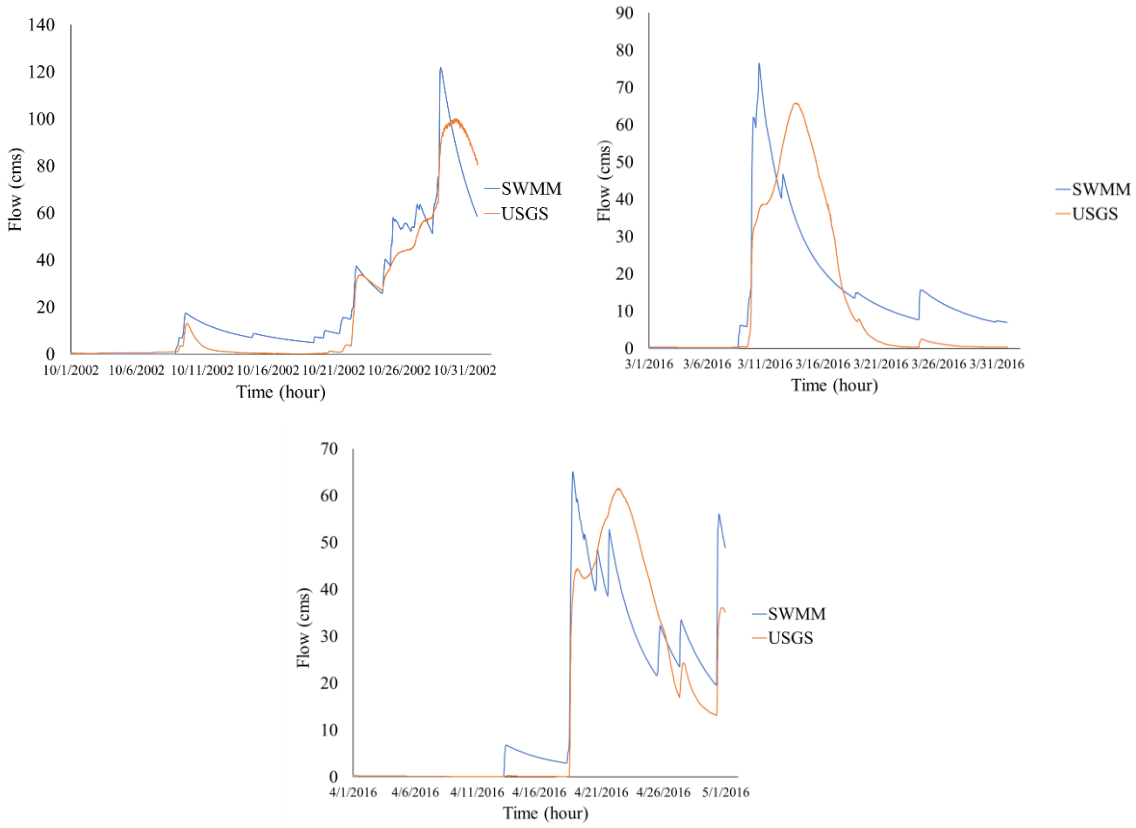

Figure 2-6. Simulated and observed flow in the test catchment within three proposed time intervals.

2.3 Development of MOPUS_S Model

The MOPUS model introduced by McCarthy et al. (2011) is a microbe model that incorporates surface and subsurface components to simulate the buildup and washing from micro-organisms. Micro-organisms obtain their food from both animals and humans. The longevity of these microbes depends on various environmental conditions, including temperature, humidity, pH, nutrition content, salinity, and toxicity, once they have been deposited. The microbes are then

moved, which is frequently accomplished by the occurrence of runoff. This analysis only considers surface storage to estimate bacteria concentration within each subcatchment. The governing equations for the micro-organism model are presented in Table 2-5 (McCarthy et al., 2011).

Table 2-5. The governing equations of the micro-organism model in MOPUS.

Model Equation	Comment
$P_s(t) = 10^{PsCoeff} \times \left[\frac{VP(t-1)}{\overline{VP}}\right]^{VPCoeff} \times \left[\frac{RH(t-1)}{\overline{RH}}\right]^{RHCoeff}$	Surface storage
$C_s(t) = \frac{P_s(t) \times RI(t)^{1.293}}{RI(t)}$	Surface wash-off

where Ps(t) indicates surface storage (orgs), VP(t−1) is previous day's vapor pressure (hpa), \bar{VP} is the mean VP(t) value (hpa), RH(t−1) represents previous day's maximum relative humidity (%), \bar{RH} is the mean RH(t) value (%), PsCoeff, VPCoeff and RHCoeff are the calibration coefficients, Cs(t) is the surface wash-off (orgs/L), and RI(t) is the routed and translated precipitation intensity (mm/min).

MOPUS_S is the name given to the semi-distributed model that was constructed in this work. MOPUS_S model augments the original MOPUS in three primary aspects: 1) taking into account the effects of land-use types on microbial accumulation; 2) coupling SWMM with MOPUS model in order to leverage the advantages of hydrological simulation; and 3) changing the constant in MOPUS to a calibration parameter in MOPUS_S in order to complete the localization of parameters. The following were the specific algorithms used by MOPUS_S:

(1) Surface storage in a single subcatchment

$$P_{si}(t) = 10^{P_{si}\,Coeff} \times \left[\frac{VP(t-1)}{\overline{VP}}\right]^{VPCoeff} \times \left[\frac{RH(t-1)}{\overline{RH}}\right]^{RHCoeff} \times S_i \quad (orgs) \tag{2-3}$$

where Psi(t) is the pollutant accumulated in the i^{th} subcatchment area, in organisms; Si is the area of the i^{th} subcatchment, in ha; PsiCoeff, VPCoeff , and RHCoeff are the calibration coefficients; VP(t-1) is the vapor pressure measured the previous day in hpa; $\overline{VP}$ is the mean vapor pressure

measured current day in hpa; RH(t-1) is the maximum relative humidity measured the previous day in percent; RH (t-1) is the mean relative humidity measured the current day in percent. The wet-bulb temperature at 9 a.m. was used to determine the vapor pressure. At the same time, the relative humidity was taken from data acquired from the meteorological station, and Si was extracted from the SWMM input.

(2) Surface wash-off in a single subcatchment

$$C_{si}(t) = \frac{P_{si}(t) \times \left[\frac{6Q_i(t)}{S_i}\right]^{C_s\ \mathrm{Coeff}}}{6 \times 10^5 Q_i(t)} \ (\mathrm{org}/100\ \mathrm{mL}) \qquad (2\text{-}4)$$

where Qi(t) is the surface runoff of the ith subcatchment, calculated from the SWMM output (converted to mL/min), and the constants in the formula are for unit conversion. The final orgs/100 mL result corresponds to our monitoring measurement of the most probable number (MPN)/100 mL, which we obtained using a titration process. The calibration parameter is represented by the symbol C_sCoeff.

While SWMM runoff simulations could not be calibrated directly due to a lack of flow observations, there is a TCEQ station number 10575 located near the downstream of the watershed whose records were used in calibrated the MOPUS_S. The station reported average concentration of fecal bacteria on 1/14/2016 and 7/19/2016 (150 and 610 organisms, respectively). Using these bacteria concentrations, the MOPU_S model has been calibrated with the favorable coefficients listed in Table 2-6. The average value of $P_{siCoeff}$ is 7.82, and it is considered for further bacteria concentration calculation.

Table 2-6. Values of the calibrated parameters for the MOPUS_S model.

Report date: 01/14/2016			
PsiCoeff	VPCoeff	RHCoeff	CsCoeff
7.7	2	2	2
Report date: 07/19/2016			
PsiCoeff	VPCoeff	RHCoeff	CsCoeff
7.94	2	2	2

It should be noted that the design storms only contain information on rainfall, whereas MOPUS_S requires additional meteorological data to run. To address this gap, the meteorological data from 08/26/2017 to 08/27/2017 were used jointly with the design hyetographs in performing the coupled simulations. This practice essentially assumes that the meteorological conditions for the design storms mimic those during Harvey, and this is a reasonable assumption considering that the August-September is the period that features many historical storms, and variations in temperature, relatively humidity, and air temperature among these events were likely small. In this study, the relative humidity and vapor pressure during Harvey are obtained from the National Solar Radiation Database and shown in Table 2-7. The sources of other input data such as precipitation is listed in Table 2-1.

Table 2-7. Hydrometeorological variables from 08/26/2017.

Date	Relative humidity of the current day	Relative humidity of the previous day	Average vapor pressure of current day (hPa)	Vapor pressure of previous day (hPa)
08/26/2017	99	98	33.25	31.31

2.4 Best Management Practice (BMP) Implementation

As indicated earlier, SWMM offers several modules for modeling small-scale, decentralized BMPs. At present, the model has the ability to account for the aggregate effects of a specific type of BMPs over each subcatchment, and does not account for the actual locations where these BMPs are implemented. Out of the eight BMP types noted earlier in the introduction part, wet detention ponds were chosen as past investigations generally pointed to their efficacy in reducing bacteria loading.

Wet ponds operate on the plug flow concept, where influent runoff enters the pond and supposedly replaces previously caught runoff. While sedimentation in wet ponds is the primary method of pollutant removal, additional processes such as oxidation-reduction reactions, plant absorption, and adsorption owing to interaction with soils, plants, and collected storm water also contribute to treatment (Hathaway et al., 2009). This analysis investigates the effectiveness of the wet detention ponds, dry detention ponds, and constructed wetland on bacteria removal. The

results show that dry detention ponds have the poorest performance among them. Pennington et al. 2003 have performed a study on the removal efficiencies of wet detention ponds and dry detention ponds for different pollutants of concern in the Rough River, a tributary of the Detroit River in southeastern Michigan. This study indicates that wet detention ponds have about % 70 removals in bacteria concentration; however, the dry detention ponds have no efficiency in removing bacteria.

In SWMM, the wet detention pond is modeled as a small reservoir with an orifice that releases water gradually. The detention ponds within each subcatchment are established in SWMM by specifying aggregate storage capacity, pond geometry, and a depth-area storage curve. In this study, each pond was trapezoid-shaped with a 3:1 side slope and a maximum depth of 12 feet. In determining the potential siting of BMPs among the subcatchments, several factors were taken into considerations: 1) locations of septic tanks over the region that may have contributed to the fecal bacteria loading along the Neches River Tidal; and 2) land cover and proximity to water body. As indicated earlier, there is a large number of septic tanks, or on-site sewage facilities (OSSFs) in the study watershed. The research team obtained a database of OSSFs compiled by TCEQ and Texas A&M AgriLife over the Coastal Zone portion of the watershed. The locations of these OSSFs can be found in **Error! Reference source not found.** and a breakdown of the number of OSSFs and over each subcatchment is shown in Table 2-8**Error! Reference source not found.**.

Table 2-8. The area and number of OSSFs in each subcatchment were obtained from TCEQ and Texas A&M AgriLife drafts coastal zone databases.

Subcatchments	Area (mi^2)	Number of OSSFs
Subcatchment 1	23.31	87
Subcatchment 2	10.87	289
Subcatchment 3	5.35	34
Subcatchment 4	2.08	119
Subcatchment 5	2.39	125
Subcatchment 6	2.87	118
Subcatchment 7	7.15	148
Subcatchment 8	15.34	9
Subcatchment 9	2.68	1
Subcatchment 10	3.91	0

Subcatchment 11	3.92	118

It is clear from Figure 1-3 and Table 2-8 that a majority of the OSSFs are concentrated over the middle portion of the watershed. Two small clusters are also evident, with one located downstream near the mainstem of Neches River, and one over the northern tip of the watershed. Given this spatial pattern, the research team devised three scenarios of BMP implementations over the region that offer high potential of reducing the bacteria load as caused by leakages from OSSFs. These scenarios are illustrated in Figure 2-7 (a-c). In Scenario 1, the detention ponds are implemented in three subcatchments with the largest number of OSSFs, namely 2,5 and 7 (Figure 2-7a). In Scenario 2, the coverage of detention ponds is expanded to five subcatchments, namely 2, 4, 5, 7, and 11 (Figure 2-7b). Scenario 3 further expands the coverage of detention ponds to seven subcatchments: 1, 2, 4, 5, 6, 7 (Figure 2-7c). These scenarios will be used in determining the tradeoffs between the reduction in flow and bacteria loading and associated costs of implementation.

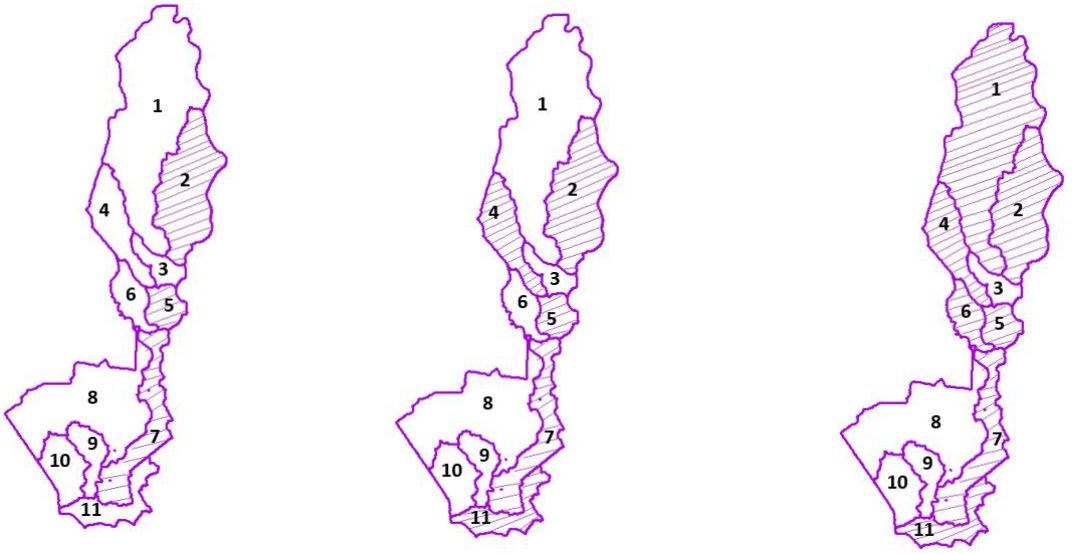

(a) First Scenario (b) Second Scenario (c) Third Scenario

Figure 2-7. Illustration of three scenarios and their included subcatchments.

2.5 Creation of storm scenarios

The construction of storm scenarios was done in two ways in the project. The first follows the standard engineering practice for deriving design storms as outlined in Chow 1962, whereas

the second one uses actual storms that took place in the region. Only the design storms were used in driving the coupled modeling system.

There are three main steps in the design storm calculation: 1) determining the duration and averaged recurrence intervals (ARIs) of interest; 2) identify the precipitation frequency estimates for the duration ARI from published intensity-duration-frequency (IDF) curves for the study watershed; and 3) disaggregate the precipitation amounts derived in 2) to finer time intervals to create design hyetographs. In this study, the duration for the design storm was chosen to be 24h given the relatively small size of the subcatchment (~80 mi^2), and three ARIs were selected, namely 25, 50 and 100 years. The 24-h totals for these durations were taken from NOAA Atlas-14 frequency maps. In engineering design, the point-wise precipitation frequency estimates are often adjusted downward to derive watershed-scale estimates through the areal reduction factor. As the watershed is relatively small, it is reasonable to assume that the adjustment factor is close to unity.

The design hyetograph can be created using methods such as the alternating block, instantaneous intensity, and triangular hyetograph (Chow, 2010). In this study, the alternating block method was chosen. This approach specifies the precipitation depth in "n" consecutive time intervals of duration (t) over a total period. The precipitation intensity is retrieved from the IDF curve for each duration from the Atlas-14 Intensity-duration-frequency curve (Butler and John, 2011). The resulting 25, 50 and 100-yr design hyetographs are shown in Figure 2-8.

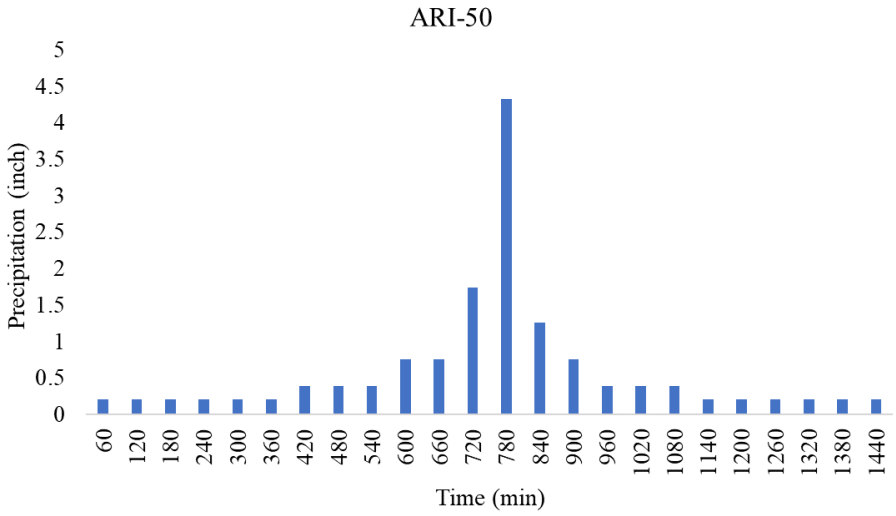

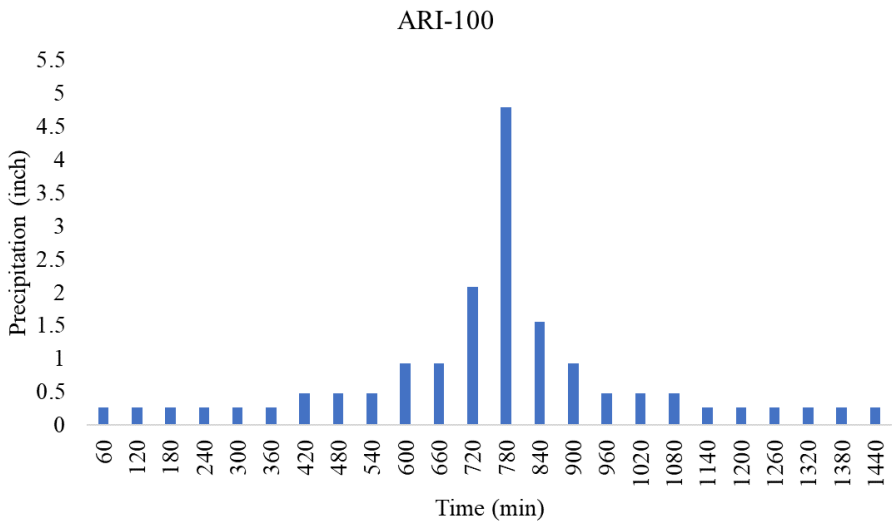

Figure 2-8 . 24-h design hyetographs for 25, 50 and 100-year average recurrence intervals.

3. RESULTS

An ensemble of scenarios with varying spatial distributions of detention ponds were created in assessing the impacts of BMPs on flow and bacteria loading. In each scenario, the BMPs for each subcatchment are assigned a prescribed total percentage area. The resulting SWMM configurations were used to perform runoff simulations with design hyetographs described earlier, and the simulated streamflow was used as input to the MOPUS_S model to produce bacteria loading. The results are compared against the baseline simulations in which no BMPs were installed.

Sensitivity analysis was performed wherein the percentage coverage of detention ponds was varied to achieve ~40% reduction inflow for 25, 50 and 100-yr design storms. The results are shown in Table 3-1.

Table 3-1. Wet detention ponds implementation percentage in the subcatchments in response to various design storms.

Sub catchment	Area (mi^2)	25-yr		50-yr		100-yr	
		Pond Area (mi^2)	Pond Area Percentage (%)	Pond Area (mi^2)	Pond Area Percentage (%)	Pond Area (mi^2)	Pond Area Percentage (%)
1	16.44	0.20	1.22	0.25	1.52	0.29	1.77
2	5.15	0.07	1.40	0.09	1.74	0.12	2.33
4	4.08	0.07	1.70	0.09	2.20	0.10	2.45
5	2.39	0.05	2.10	0.07	2.92	0.07	2.93
6	2.87	0.05	1.74	0.07	2.44	0.08	2.78
7	7.15	0.12	1.80	0.15	2.10	0.18	2.52
11	3.92	0.06	1.53	0.07	1.78	0.09	2.29

It should be noted that the sizes of BMPs increase for more intense storms to achieve comparable levels of reduction in runoff peak.

3.1 Impacts of BMPs on runoff

Table 3-2 illustrates the performance of BMPs for mitigation of the peak flow under various design storms. Figure 3-1 illustrates changes in the shape of runoff hydrographs after applying the detention ponds for subcatchments 1, 2, 4, 5, 6, 7, and 11 using 25-yr ARI design storm. Also, the impacts of detention ponds for 50-yr, and 100-yr ARI design storms are illustrated in Figures 3-2

and 3-3. It is evident that the introduction of detention not only reduces the peak flow but also considerably retards the flow locally.

Table 3-2. Peak flow reduction after BMPs implementation in the subcatchments for 25-yr, 50-yr, and 100-yr design storms.

	25-yr		50-yr		100-yr	
Sub catchment	Peak Flow before/ after BMP (CMS)	Percent Reduction (%)	Peak Flow before/after BMP (CMS)	Percent Reduction (%))	Peak Flow before/after BMP (CMS)	Percent Reduction (%)
1	160/100	37.50	220/140	36.40	275/180	35.00
2	88/55	37.50	110/70	36.50	140/90	36.00
4	60/38	36.70	78/50	35.90	100/60	40.00
5	50/30	40.00	65/40	38.50	80/50	37.50
6	32/18	43.75	42/27	35.70	55/35	35.00
7	62/40	35.50	80/50	37.50	105/65	38.00
11	105/65	38.00	130/80	38.50	152/98	35.00

Table 3-3. Peak flow in the watershed outlet before and after BMPs implementation and associated reduction under third scenario.

Design Storm	Peak flow before BMPs (CMS)	Peak flow after BMPs (CMS)	Percent reduction (%)
25-yr	1118	841	24.70
50-yr	1600	1200	25.00
100-yr	1850	1370	25.50

The result of this analysis indicates that the peak flow reduction in the watershed outlet under the third scenario is estimated to be roughly 25 percent as shown in Table 3-3.

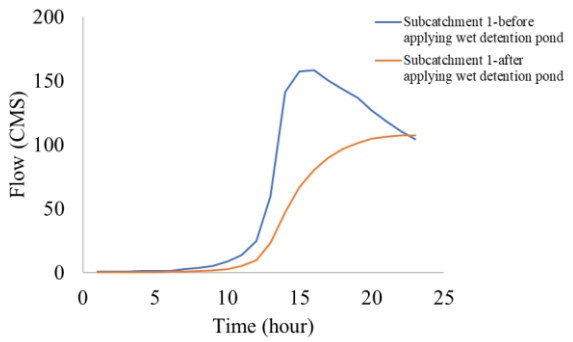
Subcatchment 1-before applying wet detention pond
Subcatchment 1-after applying wet detention pond
Flow (CMS)
Time (hour)

(a)

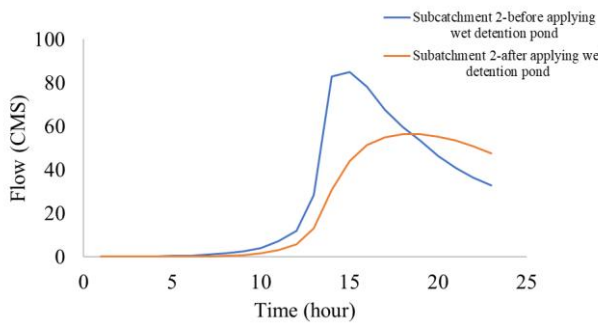
Subcatchment 2-before applying wet detention pond
Subatchment 2-after applying we detention pond
Flow (CMS)
Time (hour)

(b)

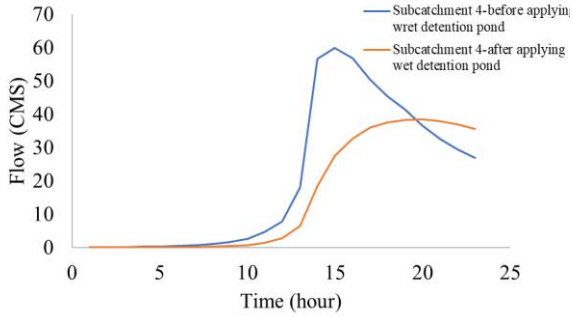
Subcatchment 4-before applyin wret detention pond
Subcatchment 4-after applying wet detention pond
Flow (CMS)
Time (hour)

(c)

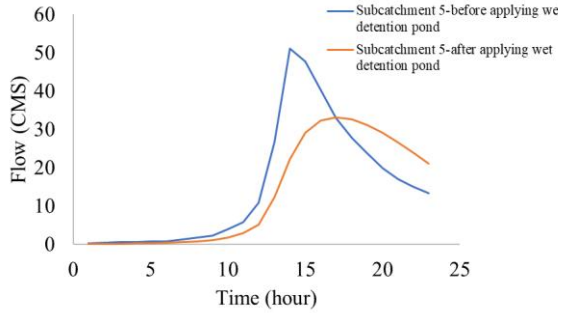
Subcatchment 5-before applying we detention pond
Subcatchment 5-after applying wet detention pond
Flow (CMS)
Time (hour)

(d)

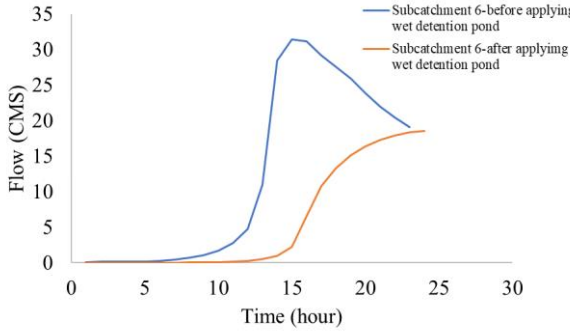
Subcatchment 6-before applyin wet detention pond
Subcatchment 6-after applyimg wet detention pond
Flow (CMS)
Time (hour)

(e)

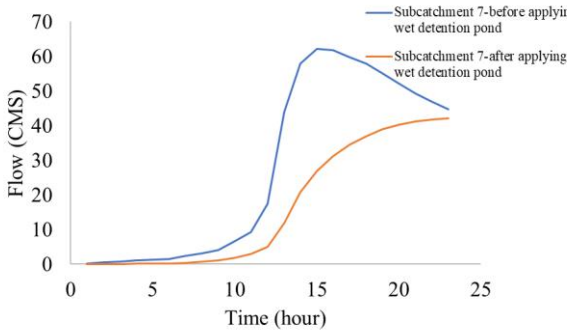
Subcatchment 7-before applyi wet detention pond
Subcatchment 7-after applying wet detention pond
Flow (CMS)
Time (hour)

(f)

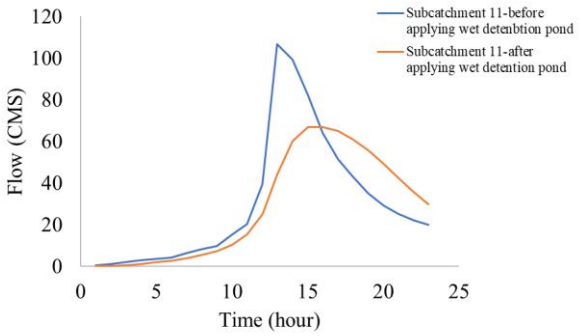

(g)

Figure 3-1. Illustration of three scenarios considering 25-yr design storm. Flow time series before and after applying wet detention ponds in the subcatchments (a) subcatchment 1, (b) subcatchment 2, (c) subcatchment 4, and (d) subcatchment 5, (e) subcatchment 6, (f) subcatchment 7, (g) subcatchment 11.

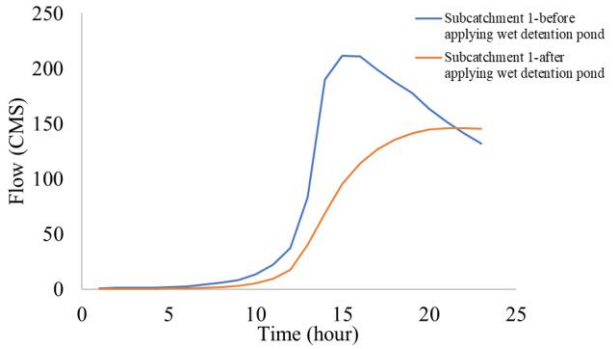

(a)

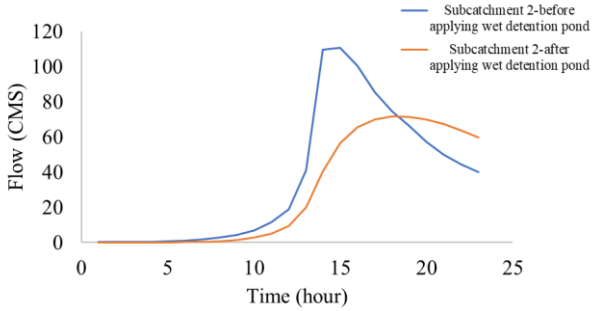

(b)

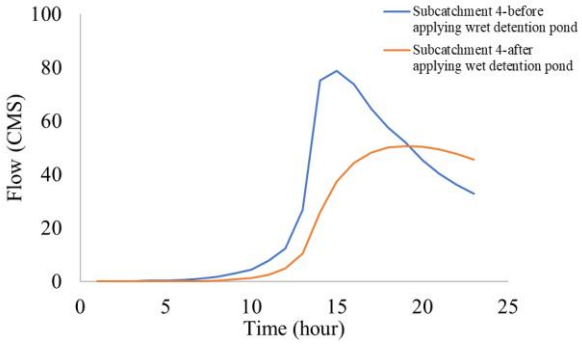

(c)

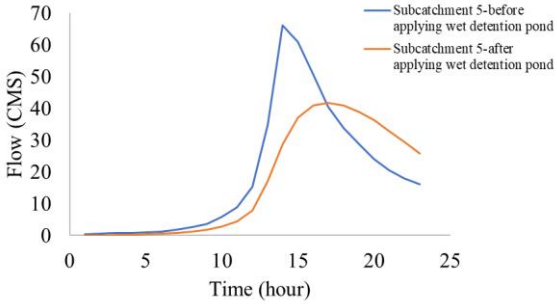

(d)

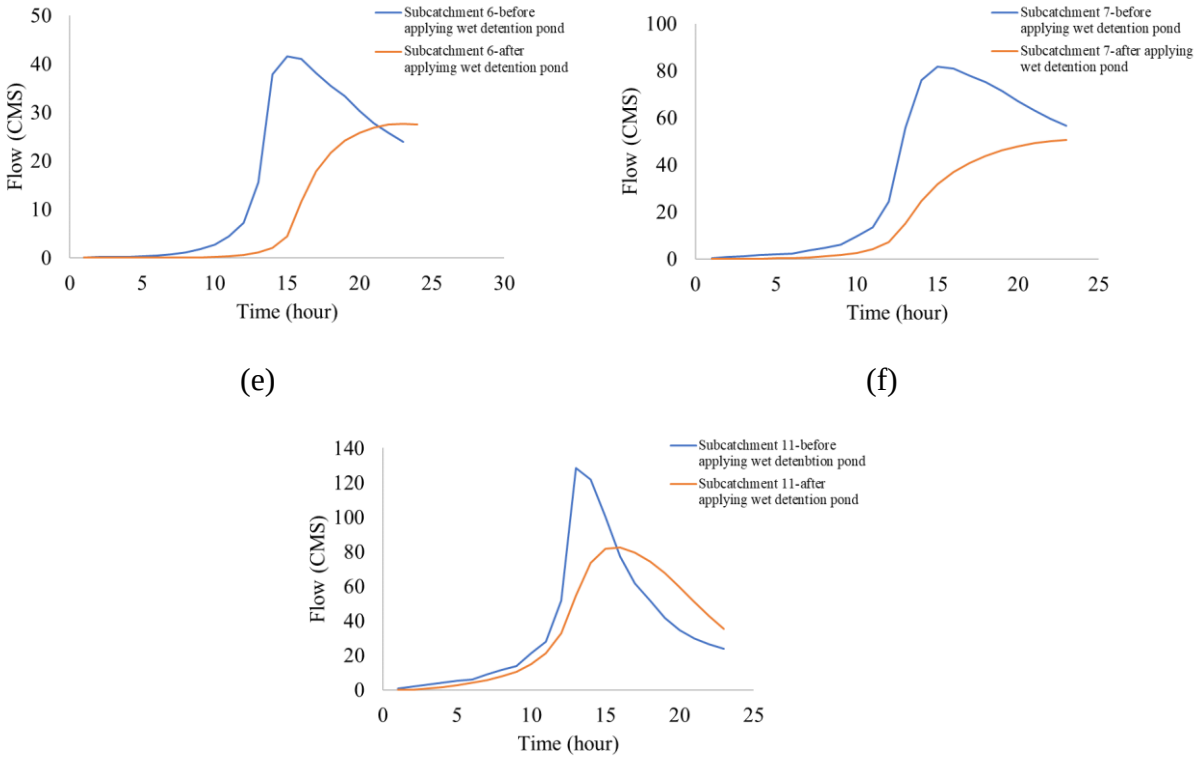

(e) (f)

(g)

Figure 3-2. Illustration of three scenarios considering 50-yr design storm. Flow time series before and after applying wet detention ponds in the subcatchments (a) subcatchment 1, (b) subcatchment 2, (c) subcatchment 4, and (d) subcatchment 5, (e) subcatchment 6, (f) subcatchment 7, (g) subcatchment 11.

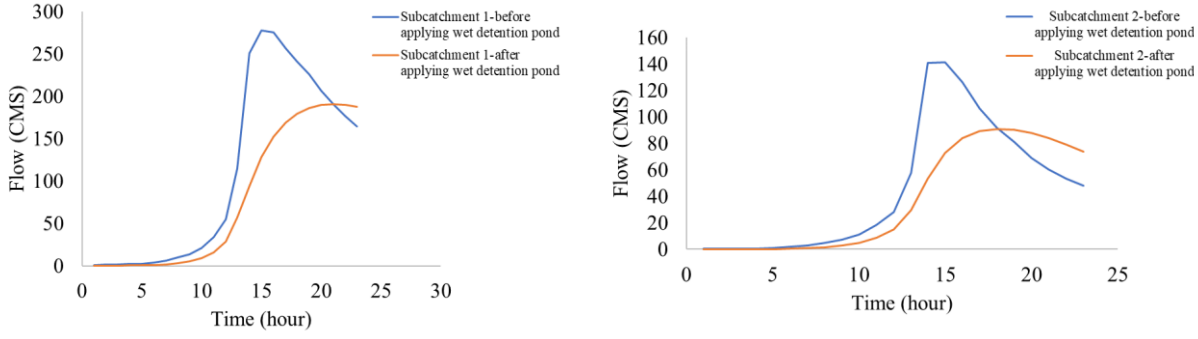

(a) (b)

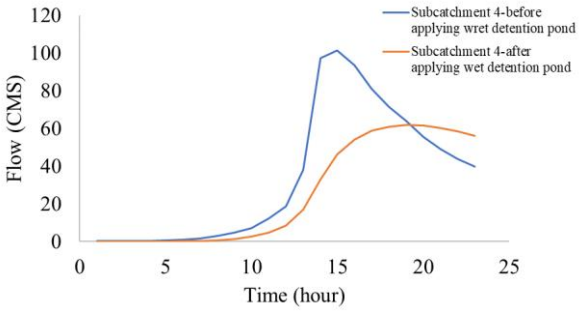

(c)

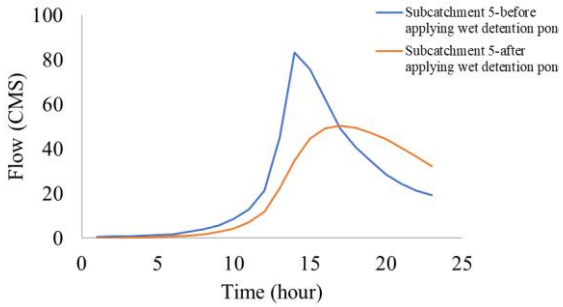

(d)

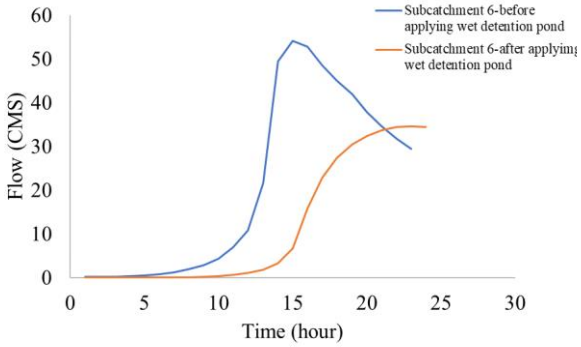

(e)

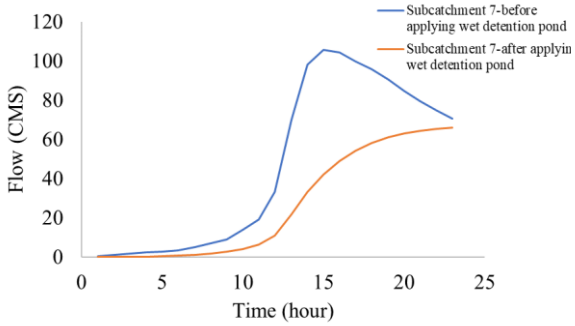

(f)

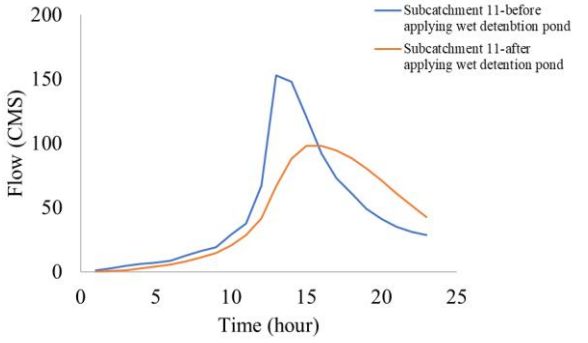

(g)

Figure 3-3. Illustration of three scenarios considering 100-yr design storm. Flow time series before and after applying wet detention ponds in the subcatchments (a) subcatchment 1, (b) subcatchment 2, (c) subcatchment 4, and (d) subcatchment 5, (e) subcatchment 6, (f) subcatchment 7, (g) subcatchment 11.

To determine the peak flow reduction in the watershed outlet after applying wet detention ponds, flow time series before and after application of these BMPs under the third scenario have been shown in Figure 3-4. As a consequence of this research, the peak flow decrease at the watershed outlet is anticipated to be about 25% under the third scenario, as seen in Fig. 3-4.

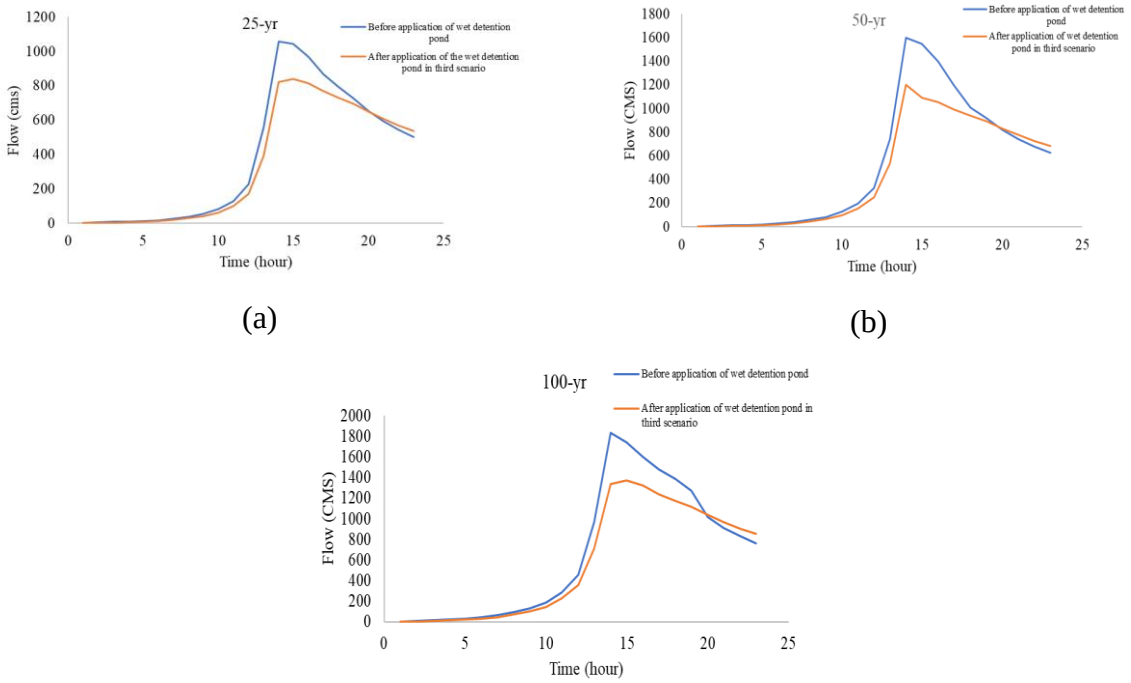

Figure 3-4. Illustration of flow time series before and after applying wet detention ponds under third scenario considering design storms. (a) 25-yr, (b) 50-yr, (c)100-yr.

3.2 Impacts of BMPs on bacteria loading

Error! Reference source not found. summarize the estimated impacts of detention on bacteria loading with 25-year, design storm for each subcatchment, and similar statistics for 50, and 100-year storms are shown in Tables 3-5 and 3-6, respectively.

The percentage reduction in bacteria loading varies among the subcatchments, with the largest reduction over subcatchment 6 and the smallest over subcatchments 1 and 7. The efficacy is the highest for the 25-year design storm and declines with the intensity of the storms. This decreasing efficacy is a reflection of the nonlinear dependence of bacteria load and peak flow.

Table 3-4. Summary of statistics of bacteria concentration for 25-yr storm design in (08/26/2017)

Subcatchments	Bacteria Concentration (before BMPs)	Bacteria Concentration (After BMPs)	Percentage Reduction
Subcatchment 1	128	87	33
Subcatchment 2	220	146	34
Subcatchment 4	195	125	36
Subcatchment 5	285	185	35
Subcatchment 6	145	86	40
Subcatchment 7	116	78	33
Subcatchment 11	362	227	37

Table 3-5. Summary of statistics of bacteria concentration for 50-yr storm design in (08/26/2017)

Subcatchments	Bacteria Concentration (before BMPs)	Bacteria Concentration (After BMPs)	Percentage Reduction
Subcatchment 1	171	118	31
Subcatchment 2	286	185	35
Subcatchment 4	256	165	36
Subcatchment 5	368	233	37
Subcatchment 6	193	128	34
Subcatchment 7	152	91	40
Subcatchment 11	437	280	36

Table 3-6. Summary of statistics of bacteria concentration for 100-yr storm design in (08/26/2017)

Subcatchments	Bacteria Concentration (before BMPs)	Bacteria Concentration (After BMPs)	Percentage Reduction
Subcatchment 1	225	154	32
Subcatchment 2	364	234	36
Subcatchment 4	330	201	40
Subcatchment 5	463	280	40
Subcatchment 6	251	158	38
Subcatchment 7	197	123	38
Subcatchment 11	519	332	36

In order to assess the cost-effectiveness of detention ponds, a cost-benefit analysis was performed wherein the costs associated with constructing the BMPs in the three implementation scenarios were calculated and compared. The costs are then compared against the percentage reduction in flow and bacteria loading. The construction cost of each detention pond is calculated using the EPA's empirical approach which relates the cost to the volume of detention, i.e., $C=29.5 V^{0.7,}$ where V is the detention pond volume (ft^3). As the empirical equation was created in 1997, the costs thus estimated were adjusted for inflation to reflect actual costs at the present time. Table

3-7, 3-8 and 3-9 show the outcomes of the cost-benefit analysis results for the three scenarios in 25-yr, 50-yr, and 100-yr design storms. In order to achieve the aforementioned percentage reduction in flow and bacteria loading for the 25-yr design storm, the costs will be $13.84M for the first scenario, $21.66M for the second scenario, and $33.97M for the third scenario. The corresponding costs for 50-yr design storm are $16.34M, $25.76M, $39.97M for the three scenarios; and for the 100-yr design storm these costs are $18.68M, $29.05M, $45.21M.

Table 3-7. Three scenarios of detention pond application and associated cost estimation and maximum flow reductions considering 25-year design storm.

First Scenario							
Subcatchments	Subcatchment Area (mi^2)	Pond Area (mi^2)	Pond Area Percentage (%)	Maximum Depth (ft)	Volume (Ac-ft)	Cost ($M)	Maximum flow reduction (%)
Subcatchment 2	5.15	0.07	1.40	12	538	4.25	38
Subcatchment 5	2.39	0.05	2.10	12	384	3.36	38
Subcatchment 7	7.15	0.12	1.80	12	929	6.23	36
Total Cost ($ M)						**13.84**	
Second Scenario							
Subcatchments	Subcatchment Area (mi^2)	Pond Area (mi^2)	Pond Area Percentage (%)	Maximum Depth (ft)	Volume (Ac-ft)	Cost ($M)	Maximum flow reduction (%)
Subcatchment 2	5.15	0.07	1.40	12	538	4.25	38
Subcatchment 4	4.08	0.07	1.70	12	500	4.00	37
Subcatchment 5	2.39	0.05	2.10	12	384	3.36	37
Subcatchment 7	7.15	0.12	1.80	12	929	6.23	36
Subcatchment 11	3.92	0.06	1.53	12	460	3.82	37
Total Cost ($ M)						**21.66**	
Third Secenario							
Subcatchments	Subcatchment Area (mi^2)	Pond Area (mi^2)	Pond Area Percentage (%)	Maximum Depth (ft)	Volume (Ac-ft)	Cost ($M)	Maximum flow reduction (%)
Subcatchment 1	16.44	0.20	1.22	12	1536	8.86	38

Subcatchment 2	5.15	0.07	1.40	12	538	4.25	38
Subcatchment 4	4.08	0.07	1.70	12	500	4.00	37
Subcatchment 5	2.39	0.05	2.10	12	384	3.36	37
Subcatchment 6	2.87	0.05	1.74	12	400	3.45	43
Subcatchment 7	7.15	0.12	1.80	12	929	6.23	36
Subcatchment 11	3.92	0.06	1.53	12	460	3.82	37
Total Cost ($ M)						**33.97**	

Table 3-8. Three scenarios of detention pond application and associated cost estimation and maximum flow reductions considering 50-yr design storm.

First Scenario							
Subcatchments	Subcatchment Area (mi2)	Pond Area (mi2)	Pond Area Percentage (%)	Maximum Depth (ft)	Volume (Ac-ft)	Cost ($M)	Maximum flow reduction (%)
Subcatchment 2	5.15	0.09	1.74	12	691	5.10	36
Subcatchment 5	2.39	0.07	2.92	12	492	4.00	38
Subcatchment 7	7.15	0.15	2.10	12	1152	7.24	38
Total Cost ($M)						**16.34**	
Second Scenario							
Subcatchments	Subcatchment Area (mi^2)	Pond Area (mi^2)	Pond Area Percentage (%)	Maximum Depth (ft)	Volume (Ac-ft)	Cost ($M)	Maximum flow reduction (%)
Subcatchment 2	5.15	0.09	1.74	12	691	5.10	36
Subcatchment 4	4.08	0.09	2.20	12	676	5.00	36
Subcatchment 5	2.39	0.07	2.92	12	492	4.00	38
Subcatchment 7	7.15	0.15	2.1	12	1152	7.24	38
Subcatchment 11	3.92	0.07	1.78	12	568	4.42	38
Total Cost ($M)						**25.76**	
Third Scenario							
Subcatchments	Subcatchment Area (mi^2)	Pond Area (mi^2)	Pond Area Percentage (%)	Maximum Depth (ft)	Volume (Ac-ft)	Cost ($M)	Maximum flow reduction (%)
Subcatchment 1	16.44	0.25	1.52	12	1882	10.21	36
Subcatchment 2	5.15	0.09	1.74	12	691	5.10	36

Subcatchment 4	4.08	0.09	2.20	12	676	5.00	36
Subcatchment 5	2.39	0.07	2.92	12	492	4.00	38
Subcatchment 6	2.87	0.07	2.44	12	500	4.00	36
Subcatchment 7	7.15	0.15	2.10	12	1152	7.24	38
Subcatchment 11	3.92	0.07	1.78	12	568	4.42	38
Total Cost ($M)						**39.97**	

Table 3-9. Three scenarios of detention pond application and associated cost estimation and maximum flow reductions considering 100-yr design storm.

First Scenario							
Subcatchments	Subcatchment Area (mi^2)	Pond Area (mi^2)	Pond Area Percentage (%)	Maximum Depth (ft)	Volume (Ac-ft)	Cost ($M)	Maximum flow reduction (%)
Subcatchment 2	5.15	0.12	2.33	12	922	6.20	36
Subcatchment 5	2.39	0.07	2.93	12	538	4.25	38
Subcatchment 7	7.15	0.18	2.52	12	1382	8.23	38
Total Cost ($ M)						**18.68**	
Second Scenario							
Subcatchments	Subcatchment Area (mi^2)	Pond Area (mi^2)	Pond Area Percentage (%)	Maximum Depth (ft)	Volume (Ac-ft)	Cost ($M)	Maximum flow reduction (%)
Subcatchment 2	5.15	0.12	2.33	12	922	6.20	36
Subcatchment 4	4.08	0.10	2.45	12	737	5.30	40
Subcatchment 5	2.39	0.07	2.93	12	538	4.25	38
Subcatchment 7	7.15	0.18	2.52	12	1382	8.23	38
Subcatchment 11	3.92	0.09	2.29	12	691	5.07	36
Total Cost ($ M)						**29.05**	
Third Scenario							
Subcatchments	Subcatchment Area (mi^2)	Pond Area (mi^2)	Pond Area Percentage (%)	Maximum Depth (ft)	Volume (Ac-ft)	Cost ($M)	Maximum flow reduction (%)
Subcatchment 1	16.44	0.29	1.77	12	2227	11.50	35

Subcatchment 2	5.15	0.12	2.33	12	922	6.20	36
Subcatchment4	4.08	0.10	2.45	12	737	5.30	40
Subcatchment 5	2.39	0.07	2.93	12	538	4.25	38
Subcatchment 6	2.87	0.08	2.78	12	614	4.66	36
Subcatchment7	7.15	0.18	2.52	12	1382	8.23	38
Subcatchment 11	3.92	0.09	2.29	12	691	5.07	36
Total Cost ($ M)						**45.21**	

4. SUMMARY AND CONCLUSIONS

The Lower Neches River between the Saltwater Barrier and I-20 is a reach that is highly vulnerable to flooding, and over the past decade the loading of fecal bacteria (enterococcus faecalis) has been rising steadily. One potential contributor to this rising trend is the increased incidence of flooding over the region that led to washoff of bacteria from point and non-point sources. Our investigation suggests that a primary probable source is on-site sewage facilities (OSSFs) that are widely present in the Orange County portion of the watershed to the east of the Neches River Tidal. These facilities are largely concentrated over the middle portion of the watershed, with smaller clusters centered near the mainstem of the Neches River and over the northern tip of the watershed. The OSSFs may release bacteria through leakages. As the leaked sewage may either enter water body through surface or subsurface flows, the OSSFs can be both non-point and point sources depending on the travel paths of the sewage and their interactions with the channel. As the OSSFs age, their potential for failure increases, and this increased risk of failure is compounded by an increase in the number of extreme rainfall events over recent years.

The damages from recent flooding events over the study region, along with the rising incidence of excessive bacteria load, had compelled the communities to seek adaptive measures to remedy their effects. This study investigated the potential of distributed BMPs to remedy the flooding as well as water quality risks. Among the BMPs, it was found that wet detention ponds are likely the most effective in removing bacteria, and our study focused on integrating hypothetical wet detention ponds into a coupled modeling framework and assessing their impacts on runoff and bacteria. The coupling framework comprises a rainfall-runoff model, namely the SWMM, and a bacteria life cycle model, MOPUS_S. The SWMM was configured to represent the watershed using 11 subcatchments. Three scenarios of BMP implementations were created within SWMM, each with a specific distribution of BMPs among the subcatchments. The density of OSSFs in the catchments is considered the main factor in prioritizing the selection of subcatchments in these scenarios. The first scenario preferentially placed the detention over subcatchments situated over the middle portion of the watershed where most of OSSFs are present, whereas the second and third scenarios involve expanding the placement of detention ponds to the lower/western, and to

the upper portions of the watersheds, respectively. These arrangements were designed to prioritize the capture and removal of fecal bacteria produced by the OSSFs.

Through sensitivity analyses using the SWMM model, the percentage areal coverage of detention was determined for 25, 50 and 100-yr design storms to achieve ~40% reduction in runoff peak for each subwatershed. The outcomes of the analyses suggest that total area of detention ponds for each subcatchment needs to reach between 1 – 3 % of subcatchment area in order to archive the target reduction in flow. Through coupled simulations using MOPUS_S, concomitant reductions in bacteria loading were determined for each BMP configuration. Our analyses indicate that the percentage reduction in bacteria loading was consistently lower than that for flow, likely a result of nonlinear dependence of bacteria concentration on flow rates as represented in the MOPUS_S model.

The cost-effectiveness of the detention was assessed by comparing the costs associated with constructing the detention within the three aforementioned scenarios. For the first implementation scenario and using 25-year design storm as input, the estimated cost is approximately $14 million, and this increases to $34 million to archive comparable reduction during a 100-year design storm. The cost increases progressively with the expansion of detention into lower and further upstream subcatchments.

The scenario and cost-benefit analyses, though preliminary and grounded on a number of simplifying assumptions, point to potential of deploying distributed BMPs at reasonable costs to reduce the flood risks and improve water quality along the lower Neches. The outcomes have been shared with regional stakeholders including the Lower Neches Valley Authority (LNVA), the city of Beaumont, and Jefferson and Orange Counties, and disseminated to the public through a website https://hydromet.uta.edu/assessment-of-stormwater-infrastructure-for-mitigating-flooding-and-non-point-source-pollution/. The co-PI for this investigation, Dr. Qian Qin, will continue to engage stakeholders through the Southeast Texas Flood Coordination Study (https://www.setxfloodcoordstudy.org/) to help the latter utilize the information in devising region-wide flood management strategies over the region.

The investigation also reveals many data and information gaps that require future works to fill. Our major recommendations include:

- Initiating flow monitoring along the Neches tributary or the mainstem of Neches River Tial near I-20. These observations will help with refining and calibrating the coupled modeling system presented in this study.
- Performing bacteria tracing to determine the impacts of OSSFs versus other plausible sources, e.g., animal waste. This will help with designing more specific, robust remedies to alleviate the rising coliform loading along the Neches.
- Expanding water quality monitoring to gather more frequent samples that can be used to assess and confirm the impacts of flooding on bacteria load. Some of the past samples showing high coliform counts were taken during relatively dry periods, and a detailed analysis of potential drivers that give rise to the anomalies will be crucial.
- Establishing pilot sites where wet detention ponds are implemented and continually monitored for their efficacy in reducing bacteria loading with different vegetation types. The results can help inform future improvements to the bioretention module in SWMM.
- Improving the MOPUS_S model to more realistically reflect the pathways through which the fecal bacteria evolve and reach stream bodies.
- Conducting field survey to determine specific locations where detention is practically feasible.

ACKNOWLEDGMENTS

Funding for this project was provided by the Texas General Land Office Coastal Management Program Cycle 24 grant. The project is a collaborative effort between Department of Civil Engineering at the University of Texas at Arlington and Department of Civil and Environmental Engineering at Lamar University.

The authors would like to thanks Michael Schramm from Texas Water Resources Institute for data and support, and Anish Jantrania and Gabriele Bonati from Texas A&M Blackland Research and Extension Center.

5. REFERENCES

Abu-Zreig, M., Rudra, R. P., Lalonde, M. N., Whiteley, H. R., & Kaushik, N. K. (2004). Experimental investigation of runoff reduction and sediment removal by vegetated filter strips. *Hydrological Processes*, *18*(11), 2029–2037.

Agriculture, U. S. D. of. (1986). Natural Resources Conservation Service. *Urban Hydrology for Small Watersheds*.

Bedan, E. S., & Clausen, J. C. (2009). Stormwater runoff quality and quantity from traditional and low impact development watersheds 1. *Jawra Journal of the American Water Resources Association*, *45*(4), 998–1008.

Berndtsson, J. C. (2010). Green roof performance towards management of runoff water quantity and quality: A review. *Ecological Engineering*, *36*(4), 351–360.

~~Birkland, T. A., Burby, R. J., Conrad, D., Cortner, H., & Michener, W. K. (2003). River ecology and flood hazard mitigation. *Natural Hazards Review*, *4*(1), 46–54.~~

Blake, E. S., & Zelinsky, D. A. (2018). National Hurricane center tropical cyclone report: Hurricane Harvey. *National Hurricane Center, National Oceanographic and Atmospheric Association*.

Chui, T. F. M., Liu, X., & Zhan, W. (2016). Assessing cost-effectiveness of specific LID practice designs in response to large storm events. *Journal of Hydrology*, *533*, 353–364.

Coombes, P. J., Argue, J. R., & Kuczera, G. (2000). Figtree Place: a case study in water sensitive urban development (WSUD). *Urban Water*, *1*(4), 335–343.

D'Arcy, B., & Frost, A. (2001). The role of best management practices in alleviating water quality problems associated with diffuse pollution. *Science of the Total Environment*, *265*(1–3), 359–367.

Davis, A. P. (2005). *Green engineering principles promote low-impact development*. ACS Publications.

Environmental Protection Agency. (2004). *Primer for Municipal Wastewater Treatment Systems*. US Environmental Protection Agency Municipal Support, Division Office of ….

Few, R. (2003). Flooding, vulnerability and coping strategies: local responses to a global threat. *Progress in Development Studies*, *3*(1), 43–58.

Gassman, P. W., Arnold, J. J., Srinivasan, R., & Reyes, M. (2010). The worldwide use of the

SWAT Model: Technological drivers, networking impacts, and simulation trends. *21st Century Watershed Technology: Improving Water Quality and Environment Conference Proceedings, 21-24 February 2010, Universidad EARTH, Costa Rica*, 1.

Gros, M., Blum, K. M., Jernstedt, H., Renman, G., Rodríguez-Mozaz, S., Haglund, P., Andersson, P. L., Wiberg, K., & Ahrens, L. (2017). Screening and prioritization of micropollutants in wastewaters from on-site sewage treatment facilities. *Journal of Hazardous Materials, 328*, 37–45.

Guto, S. N., Pypers, P., Vanlauwe, B., de Ridder, N., & Giller, K. E. (2011). Tillage and vegetative barrier effects on soil conservation and short-term economic benefits in the Central Kenya highlands. *Field Crops Research, 122*(2), 85–94.

Hamel, P., Daly, E., & Fletcher, T. D. (2013). Source-control stormwater management for mitigating the impacts of urbanisation on baseflow: A review. *Journal of Hydrology, 485*, 201–211.

Harrell, L. J., & Ranjithan, S. R. (2003). Detention pond design and land use planning for watershed management. *Journal of Water Resources Planning and Management*, *129*(2), 98–106.

Hathaway, J. M., Hunt, W. F., & Jadlocki, S. (2009). Indicator bacteria removal in storm-water best management practices in Charlotte, North Carolina. Journal of Environmental Engineering, 135(12), 1275-1285.

Haydon, S., & Deletic, A. (2006). Development of a coupled pathogen-hydrologic catchment model. *Journal of Hydrology*, *328*(3–4), 467–480.

He, L.-M. L., & He, Z.-L. (2008). Water quality prediction of marine recreational beaches receiving watershed baseflow and stormwater runoff in southern California, USA. *Water Research*, *42*(10–11), 2563–2573.

Hegar, G. (2018). *A storm to remember*.

https://www.weather.gov/media/hgx/climate/summary/August_Climate_Article_2012.pdf. (n.d.).

Hou, X., Chen, L., Qiu, J., Zhang, Y., & Shen, Z. (2019). A Semi-distributed Model for Predicting Faecal Coliform in Urban Stormwater by Integrating SWMM and MOPUS. International journal of environmental research and public health, 16(5), 847.

James, R. J. E., & Ferguson, E. (2020). The dynamic relationship between pain, depression and cognitive function in a sample of newly diagnosed arthritic adults: a cross-lagged panel

model. *Psychological Medicine*, *50*(10), 1663–1671.

Jang S et al (2007) Using SWMM as a tool for hydrologic impact assessment. Desalination 212:344–356

Karamouz, M, Taheri, M., Mohammadi, K., Heydari, Z., & Farzaneh, H. (2018). A New Perspective on BMPs' Application for Coastal Flood Preparedness. *World Environmental and Water Resources Congress 2018*, 171–180. https://doi.org/10.1061/9780784481431.018

Karamouz, Mohammad, & Farzaneh, H. (2020). Margin of Safety Based Flood Reliability Evaluation of Wastewater Treatment Plants: Part 2-Quantification of Reliability Attributes. *Water Resources Management*, *34*, 2043–2059.

Karamouz, Mohammad, Farzaneh, H., & Dolatshahi, M. (2020). Margin of Safety Based Flood Reliability Evaluation of Wastewater Treatment Plants: Part 1 – Basic Concepts and Statistical Settings. *Water Resources Management*, *34*(2), 579–594. https://doi.org/10.1007/s11269-019-02465-8

Kim, M. H., Sung, C. Y., Li, M.-H., & Chu, K.-H. (2012). Bioretention for stormwater quality improvement in Texas: Removal effectiveness of Escherichia coli. *Separation and Purification Technology*, *84*, 120–124.

Kossin, J. P. (2018). A global slowdown of tropical-cyclone translation speed. *Nature*, *558*(7708), 104–107.

~~Lavers, D. A., Ralph, F. M., Waliser, D. E., Gershunov, A., & Dettinger, M. D. (2015). Climate change intensification of horizontal water vapor transport in CMIP5. *Geophysical Research Letters*, *42*(13), 5617–5625.~~

Liu, R., Zhang, P., Wang, X., Chen, Y., & Shen, Z. (2013). Assessment of effects of best management practices on agricultural non-point source pollution in Xiangxi River watershed. *Agricultural Water Management*, *117*, 9–18.

McCarthy, D. T., Deletic, A., Mitchell, V. G., & Diaper, C. (2011). Development and testing of a model for Micro-Organism Prediction in Urban Stormwater (MOPUS). *Journal of Hydrology*, *409*(1–2), 236–247.

McCarthy, D. T., Mitchell, V. G., Deletic, A., & Diaper, C. (2007). Escherichia coli in urban stormwater: explaining their variability. *Water Science and Technology*, *56*(11), 27–34.

McIntyre, J. K., Davis, J. W., Hinman, C., Macneale, K. H., Anulacion, B. F., Scholz, N. L., & Stark, J. D. (2015). Soil bioretention protects juvenile salmon and their prey from the toxic

impacts of urban stormwater runoff. *Chemosphere*, *132*, 213–219.

Morrison, D. (2014). *Quantifying E. coli Discharge from Failing Onsite Sewage Facilities in the Dickinson Bayou Watershed, Texas*.

Muthukrishnan, Swama, Richard, F., & Sullivan, D. (2006). Types of best management practices. *The Use of Best Management Practices (BMPs) in Urban Watersheds*, 21–77.

Muthukrishnan, Swarna, & Selvakumar, A. (2006). Evaluation of retention pond and constructed wetland BMPs for treating particulate-bound heavy metals in urban stormwater runoff. *World Environmental and Water Resource Congress 2006: Examining the Confluence of Environmental and Water Concerns*, 1–13.

Napier, F., Jefferies, C., Heal, K. V, Fogg, P., Arcy, B. J. D., & Clarke, R. (2009). Evidence of traffic-related pollutant control in soil-based Sustainable Urban Drainage Systems (SUDS). *Water Science and Technology*, *60*(1), 221–230.

Nielsen-Gammon, J., Escobedo, J., Ott, C., Dedrick, J., & Van Fleet, A. (2020). Assessment of Historic and Future Trends of Extreme Weather in Texas, 1900-2036.

Panagopoulos, Y., Makropoulos, C., & Mimikou, M. (2011). Reducing surface water pollution through the assessment of the cost-effectiveness of BMPs at different spatial scales. *Journal of Environmental Management*, *92*(10), 2823–2835.

Park S, Lee K, Park I, Ha S (2008) Effect of the aggregation level of surface runoff fields and sewer network for a SWMM simulation. Desalination 226:328–33

Reed, Stowe, and Yanke, LLC. (2001). *Study to Determine the Magnitude of, and Reasons for, Chronically Malfunctioning On-site Sewage Facility Systems in Texas.* URL: <www.tceq.texas.gov/assets/public/compliance/compliance_support/regulatory/ossf/StudyToDetermine.pdf>

Roesner, L. A., Bledsoe, B. P., & Brashear, R. W. (2001). Are best-management-practice criteria really environmentally friendly? *Journal of Water Resources Planning and Management*, *127*(3), 150–154.

Rossman, L. A. (2010). *Storm water management model user's manual, version 5.0*. National Risk Management Research Laboratory, Office of Research and ….

Roy, A. H., Wenger, S. J., Fletcher, T. D., Walsh, C. J., Ladson, A. R., Shuster, W. D., Thurston, H. W., & Brown, R. R. (2008). Impediments and solutions to sustainable, watershed-scale urban stormwater management: lessons from Australia and the United States. *Environmental*

Management, *42*(2), 344–359.

Scholz, M., & Grabowiecki, P. (2007). Review of permeable pavement systems. *Building and Environment*, *42*(11), 3830–3836.

Shaver, E., Horner, R. R., Skupien, J., May, C., & Ridley, G. (2007). *Fundamentals of urban runoff management: Technical and institutional issues*. North American Lake Management Society.

Shaw, D. (2003). *EPA's Report on the Environment (2003 Draft)*.

Srivastava, P., Hamlett, J. M., Robillard, P. D., & Day, R. L. (2002). Watershed optimization of best management practices using AnnAGNPS and a genetic algorithm. *Water Resources Research*, *38*(3), 1–3.

Strauss, P., Leone, A., Ripa, M. N., Turpin, N., Lescot, J., & Laplana, R. (2007). Using critical source areas for targeting cost-effective best management practices to mitigate phosphorus and sediment transfer at the watershed scale. *Soil Use and Management*, *23*, 144–153.

Te Chow, V. (2010). *Applied hydrology*. Tata McGraw-Hill Education.

Vijayaraghavan, B., Ely, D. R., Chiang, Y.-M., García-García, R., & García, R. E. (2012). An analytical method to determine tortuosity in rechargeable battery electrodes. *Journal of The Electrochemical Society*, *159*(5), A548.

Vineyard, D., Ingwersen, W. W., Hawkins, T. R., Xue, X., Demeke, B., & Shuster, W. (2015). Comparing green and grey infrastructure using life cycle cost and environmental impact: A rain garden case study in Cincinnati, OH. *JAWRA Journal of the American Water Resources Association*, *51*(5), 1342–1360.

Vitro, K. A., BenDor, T. K., Jordanova, T. V, & Miles, B. (2017). A geospatial analysis of land use and stormwater management on fecal coliform contamination in North Carolina streams. *Science of The Total Environment*, *603*, 709–727.

Vis, M., Klijn, F., De Bruijn, K. M., & Van Buuren, M. (2003). Resilience strategies for flood risk management in the Netherlands. International journal of river basin management, 1(1), 33-40.

Wang Y, Sun M, Song B (2017) Public perceptions of and willingness to pay for sponge city initiatives in China resources. Conserv Recycl 122:11–20.

Zhen, X.-Y. "Jenny," Yu, S. L., & Lin, J.-Y. (2004). Optimal location and sizing of stormwater basins at watershed scale. *Journal of Water Resources Planning and Management*, *130*(4), 339–347.